Mid America Earthquake Center

Final Report for SG-4
Characterization of Active Faults in the New Madrid Seismic Zone

By
Roy Van Arsdale and Michael Ellis
Center for Earthquake Research and Information
The University of Memphis

Characterization of Active Faults in the New Madrid Seismic Zone

This is a final report that discusses the results of the Mid America Earthquake Center study SG-4 entitled, Characterization of Active Faults in the New Madrid Seismic Zone. Part one is entitled Late Cretaceous and Cenozoic Geology of the New Madrid seismic zone and Part two is entitled Forward Modeling of the Rupture Scenario of the 1811-1812 New Madrid Earthquakes. Part one discusses the geology of the New Madrid seismic zone and provides a geologic framework within which seismological, fault, and engineering characteristics are constrained. Part one also presents a tectonic model for the New Madrid seismic zone wherein the upper Mississippi Embayment is undergoing regional differential uplift. This differential uplift appears to be responsible for different faults becoming active and deactivated through time and thus provides us with a better understanding of fault behavior through time and space. Part two of this report illustrates potential rupture scenarios for the 1811-1812 earthquake sequence. Scenarios are based on the numerical modeling of a combination of historical and geological descriptions of ground deformation after the three main earthquakes. The preferred rupture scenarios suggest to us that the currently aseismic Bootheel lineament was the location of the first main rupture, and that subsequent ruptures involved the currently seismic portions of the New Madrid seismic zone. These two studies contribute significantly towards our MAE Center goal of characterizing active faults in the New Madrid seismic zone.

Acknowledgements

This research is supported by the Mid-America Earthquake Center under National Science Foundation Grant EEC-9701785. We wish to thank Richard Dart, Jodi Purser, James Dorman, Yong Li, Gerard Gonthier, Kevin Cole, Devlin Fung, Randel Cox, Martitia Tuttle, Paul Bodin, and Bill Thomas for their help in these projects.

Part 1: Late Cretaceous and Cenozoic Geology of the New Madrid Seismic Zone

Abstract

Structure contour maps constructed from well, seismic reflection, and outcrop data of the tops of the Paleozoic section, Upper Cretaceous section, Paleocene Midway Group, and Eocene section illustrate the post-Paleozoic structure of the New Madrid seismic zone region. Isopach maps of the Late Cretaceous section, Midway Group, and Eocene section help constrain the timing of the structural events. These maps, which encompass much of the northern Mississippi embayment, reveal reactivation of the underlying late Precambrian/Cambrian Reelfoot rift during Midway Group deposition but no reactivation during Late Cretaceous or Eocene deposition. The structure contour maps also indicate a subtle, south-plunging depression on the tops of the Paleozoic, Upper Cretaceous, and Midway Group along the axis of the northern Mississippi embayment that we have called a trench. This trench is 50 km wide, has a maximum depth of 100 m, and appears to have formed during the Eocene. The trench's western boundary coincides with the Blytheville arch/Lake County uplift and its southeastern margin underlies Memphis, Tennessee. The Blytheville arch/Lake County uplift is the structure responsible for the New Madrid seismic zone and thus it is possible that the southeastern margin of the trench is also a

fault zone.

A structure-contour map of the unconformity between Eocene strata and the overlying Quaternary Mississippi River alluvium of the eastern lowlands reveals relief that mirrors 1811-1812 surface coseismic deformation. We interpret the structure contour map as representing the Late Wisconsin to present strain field of the New Madrid seismic zone. This map provides constraints for future kinematic analyses of late Quaternary New Madrid faulting and allows forecasting of future coseismic deformation.

Northern Mississippi embayment post-Paleozoic stratigraphy consists of sands, silts, and clays that thicken from 477 m at New Madrid, Missouri, to 987 m near Memphis, Tennessee. The uniformity of these sediments indicates their elastic properties and therefore seismic velocities are very similar; however, variations in cementation and unconformities within the section may influence seismic wave propagation.

Introduction

Earthquakes of the New Madrid seismic zone occur within Precambrian and lower Paleozoic strata at depths between 4 and 12 km beneath the northern portion of the Mississippi embayment (Fig. 1). The Mississippi embayment is a southwest plunging trough of late Cretaceous and Tertiary age (1,2). Formation of the Mississippi embayment has been attributed to the opening of the Gulf of Mexico and reactivation of the underlying late Precambrian to Cambrian Reelfoot rift (3,4,5,6). However, Cox and Van Arsdale (7) argue that the Mississippi embayment formed as a consequence of plate tectonic drifting of the Mississippi Valley over the Bermuda hotspot in the Late Cretaceous. During early Late Cretaceous the Bermuda hotspot thermally lifted the central and southern Mississippi River Valley region and formed a north-trending arch from which a minimum of 2 km of Paleozoic strata were eroded (7). When the North American plate drifted west, off of the hotspot during the middle Late Cretaceous, the denuded Mississippi Valley region cooled and subsided to form the Mississippi embayment trough. As a consequence of the subsidence, the Mississippi embayment is filled with 900 m of Late Cretaceous and Cenozoic sediments along its axis at Memphis, Tennessee.

Numerous articles have addressed the Late Cretaceous and Cenozoic geology of the northern Mississippi embayment (NME) (8,9,1,2,10,11,12,13,14,15,16,17,18,19). In this paper we summarize the Late Cretaceous and Cenozoic geology of the NME and with a new data set present new structure contour and isopach maps of a portion of the NME centered on the New Madrid seismic zone. These data contribute to our understanding of the structure of the NME and also provide thicknesses, distributions, and compositions of the Late Cretaceous and Cenozoic embayment sediments that will affect seismic wave propagation and ground motion in the event of a large New Madrid earthquake. We hope these data will provide a geologic framework for future seismologic and engineering studies within the New Madrid seismic zone.

Construction of Structure Contour and Isopach Maps

Well log, seismic reflection, and outcrop data were collected within a 2^0 by 2^0 block (Fig. 1) centered on the New Madrid seismic zone for the elevations of the tops of the Paleozoic section, Late Cretaceous section, early to late Paleocene Midway Group, and the late Paleocene

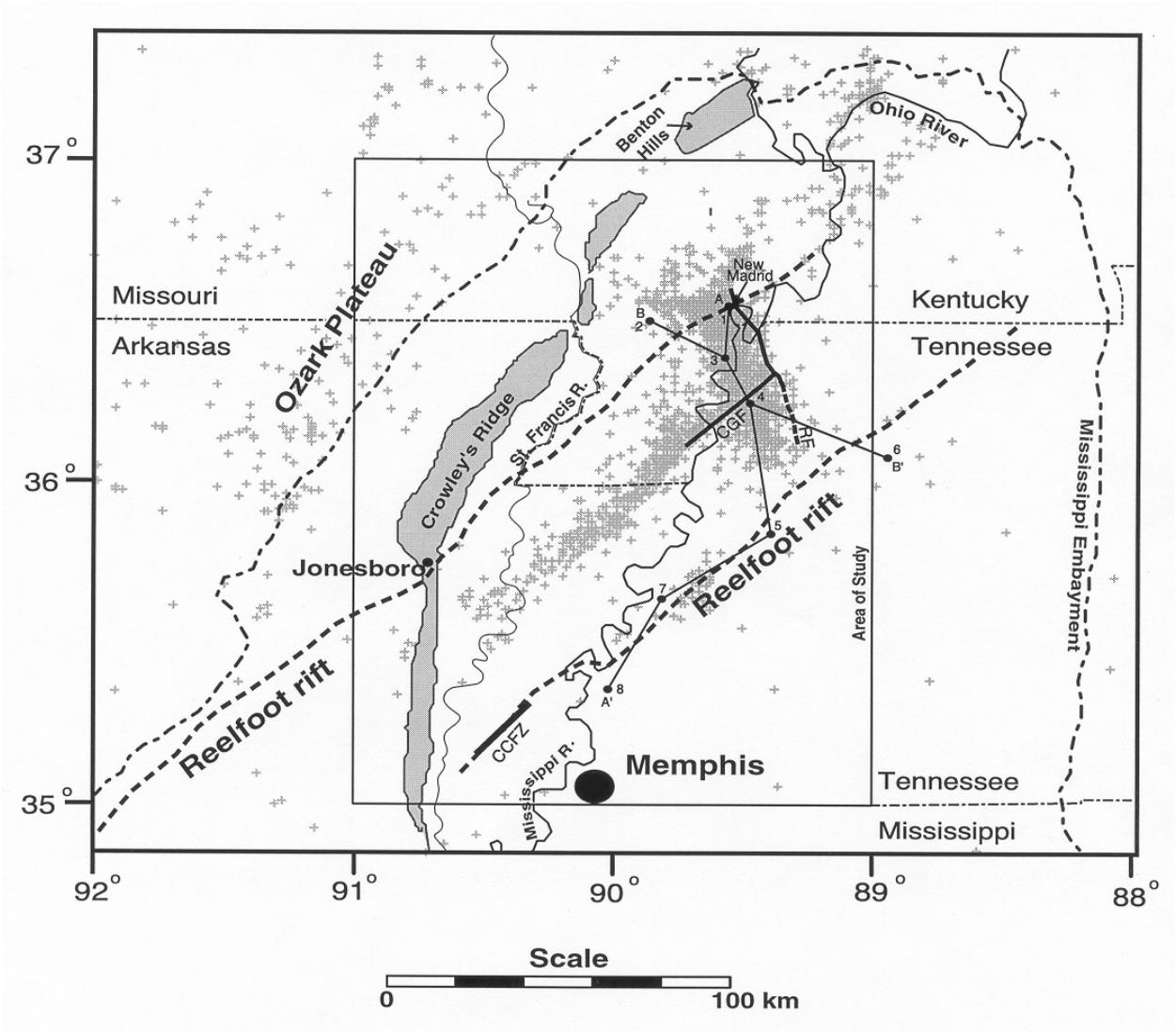

Figure 1. Major physiographic and structural features of the northern Mississippi embayment. Cross sections A-A' and B-B' are illustrated in Figure 8. Crosses locate microearthquakes that define the New Madrid seismic zone. The interior box is the area covered in Figures 3-7. CCFZ = Crittenden County fault zone, CGF = Cottonwood Grove Fault, RF = Reelfoot fault.

through early Oligocene section (Fig. 2) (see 20 for data sources and procedures). The late Paleocene through early Oligocene section consists of the Wilcox Group, Claiborne Group, and Jackson Formation. For the sake of brevity, we herein refer to the Wilcox Group through Jackson Formation as the Eocene section. Well and outcrop data, and elevations calculated from the seismic reflection data (20) were combined into one data set for each stratigraphic top; and structure contour maps were constructed using the mapping software **Surfer for Windows 6.0** by Golden Software, Inc. (Figs. 3-6). Interval velocities used in the conversion of time to depth in the seismic reflection lines were: 1821 m/sec for the interval from the top of the Midway Group to the ground surface, 1940 m/sec for the interval from the top of the Cretaceous to the top of the Midway Group, and 2000 m/sec for the interval from the top of the Paleozoic to the top of the Cretaceous. The Delaunay Triangulation with linear interpolation gridding algorithm was used in the contouring (21). Triangulation with linear interpolation was selected because it is an exact interpolator (data points coinciding with grid nodes are honored exactly), and because this method can preserve breaks in lines (faults) where data density on both sides of the fault is fairly high (21). Isopach maps (Fig. 7) of the Late Cretaceous section, the Midway Group, and the Eocene section were created by subtracting respective elevation grid files and then contouring the resultant grid files using Delaunay Triangulation.

Post-Paleozoic Stratigraphy of the Northern Mississippi Embayment

The modern Gulf Coast region is an analog for Late Cretaceous and Cenozoic sedimentation in the Mississippi embayment. Physiographically the modern Mississippi embayment and northern Gulf Coast are broadly divided into the Mississippi River flood plain, the Mississippi River delta plain, coastal shoreline east and west of the Mississippi River, near-shore marine, and deep marine. Each of these environments is dominated by particular sediments. These same types of sediments occur in the Late Cretaceous and Tertiary section of the Mississippi embayment. As sea level rose and fell during the Late Cretaceous and Tertiary the shoreline of the Gulf of Mexico, and all of its associated depositional environments, migrated north and south respectively into the NME. Thus, the lateral and vertical distribution of these Late Cretaceous and Tertiary depositional environments and their associated sediment types is complex.

In the following discussion we summarize the Late Cretaceous through Cenozoic stratigraphy of the northern Mississippi embayment (Figs. 1, 2, and 8) (22). The north-south cross section line (A-A' in Figs. 1 and 8) is discussed in detail because it trends down the axis of the NME and because it illustrates the post-Paleozoic stratigraphy from the central portion of the New Madrid seismic zone to near Memphis, Tennessee. Stratigraphy of the east-west cross section is essentially the same as the north-south cross section (Fig. 8).

Late Cretaceous Depositional History

Upper Cretaceous sediments unconformably overlie lower Paleozoic strata as old as Cambrian Knox Group in the NME (11,7). The Late Cretaceous sea transgressed from southeast to northwest, therefore, the basal Cretaceous sediments are older at the southern margin of the NME (Fig. 8). In Shelby County, Tennessee, the Coffee Formation overlies the Paleozoic unconformity (Fig. 2) (22). The Coffee Formation is a well-sorted, loose-to-friable sand that is

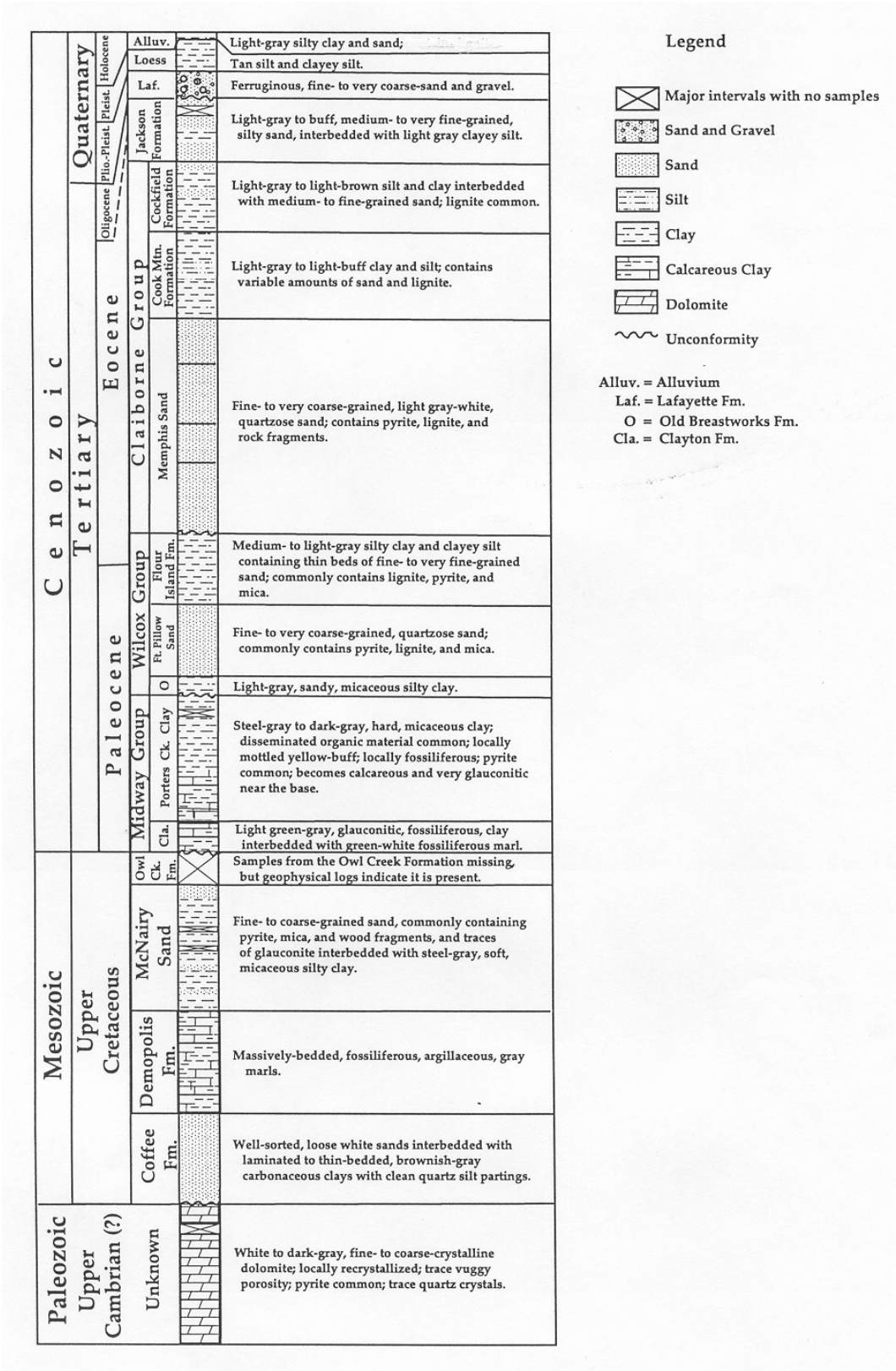

Figure 2. Geologic column for the New Madrid seismic zone (22).

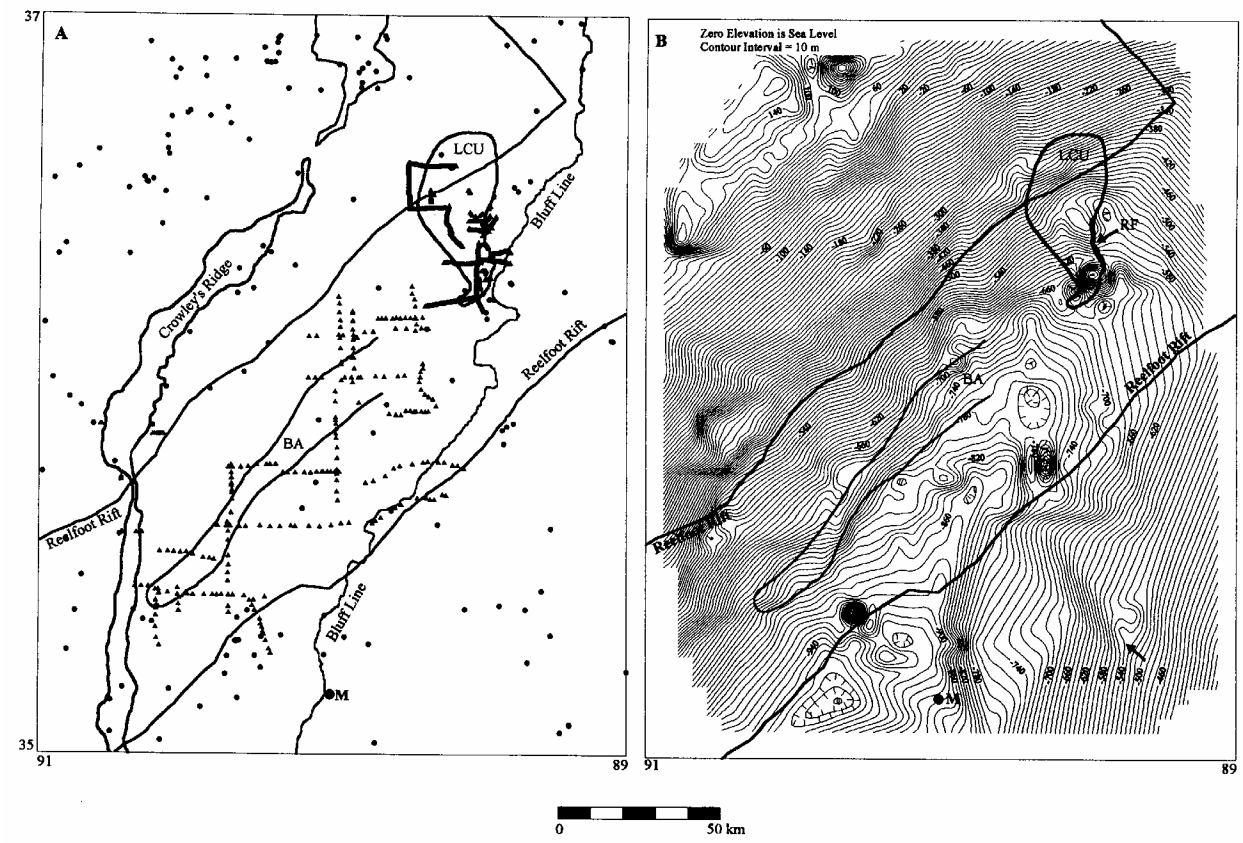

Figure 3. Data (A) and structure contour map (B) of the top of the Paleozoic strata (20). See Figure 1 for location within the Mississippi embayment. In A, the dots represent wells, triangles are depths determined from seismic reflection lines, and the solid lines are depths determined from closely-spaced reflection line data. M = Memphis, LCU = Lake County uplift, BA = Blytheville arch. Arrow indicates flexure in contour lines that may be a fault.

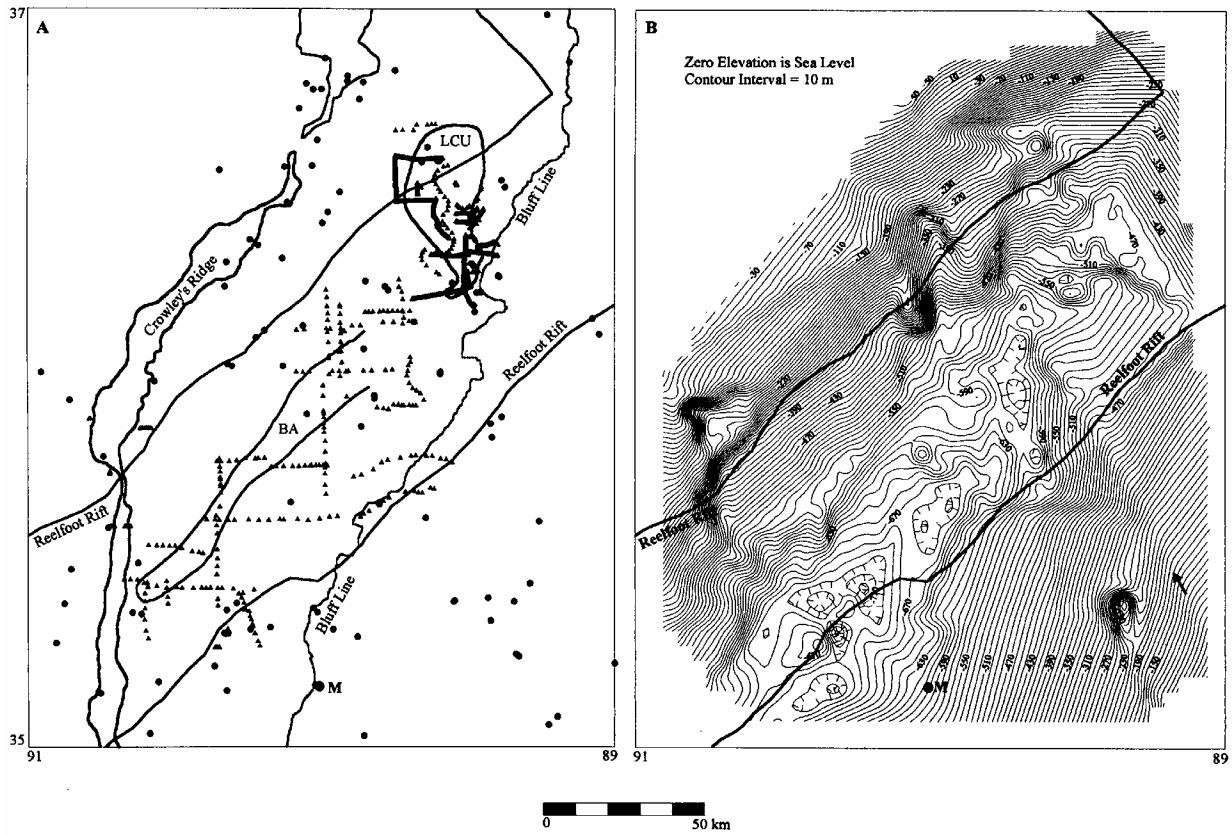

Figure 4. Data (A) and structure contour map (B) of the top of the Upper Cretaceous strata (20). See Figure 1 for location within the Mississippi embayment. In A, the dots represent wells, triangles are depths determined from seismic reflection lines, and the solid lines are depths determined from closely-spaced reflection line data. M = Memphis, LCU = Lake County uplift, BA = Blytheville arch. Arrow indicates flexure in contour lines that may be a fault.

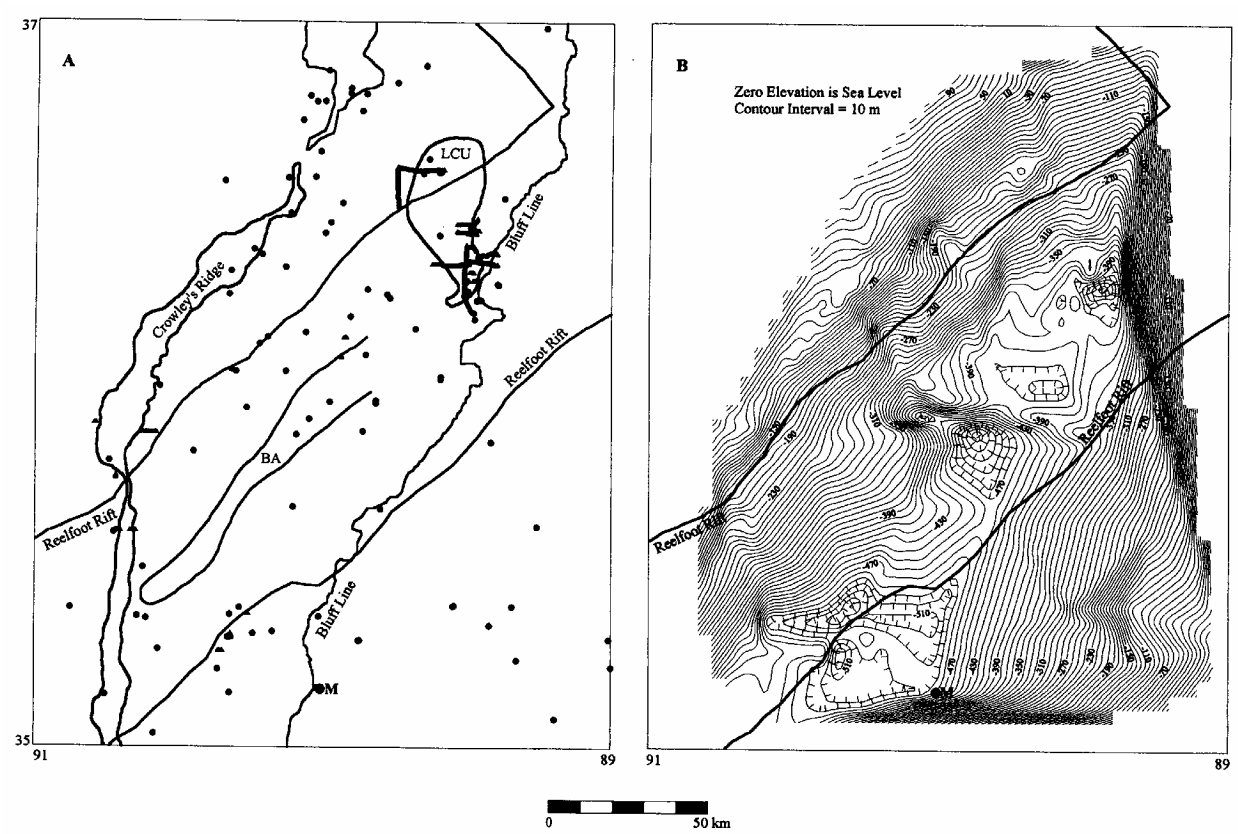

Figure 5. Data (A) and structure contour map (B) of the top of the Paleocene Midway Group (20). See Figure 1 for location within the Mississippi embayment. In A, the dots represent wells and the solid lines are depths determined from closely-spaced seismic reflection line data. M = Memphis, LCU = Lake County uplift, BA = Blytheville arch.

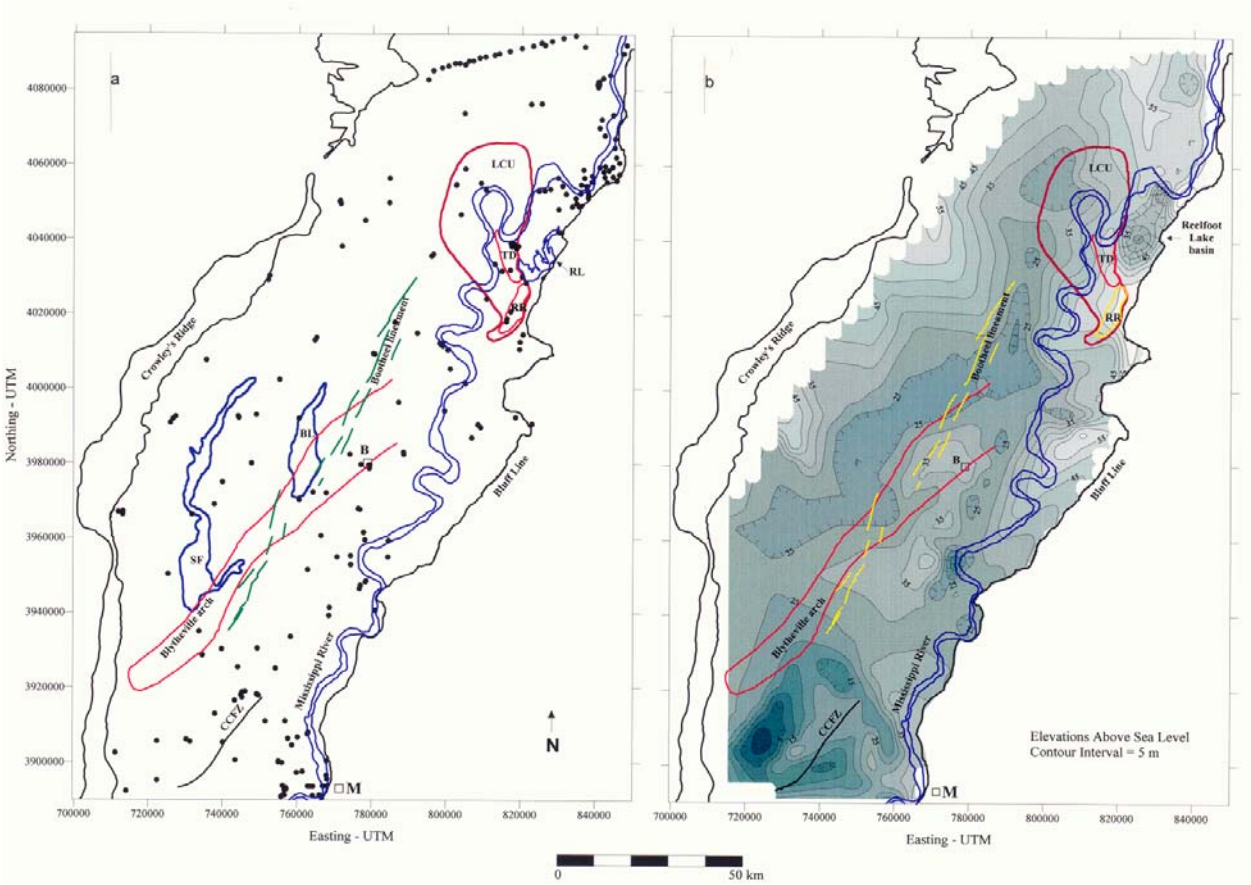

Figure 6. Data (A) and structure contour map (B) of the top of the Eocene strata (20). See Figure 1 for location within the Mississippi embayment. The dots in A represent wells. M = Memphis, LCU = Lake County uplift, BA = Blytheville arch.

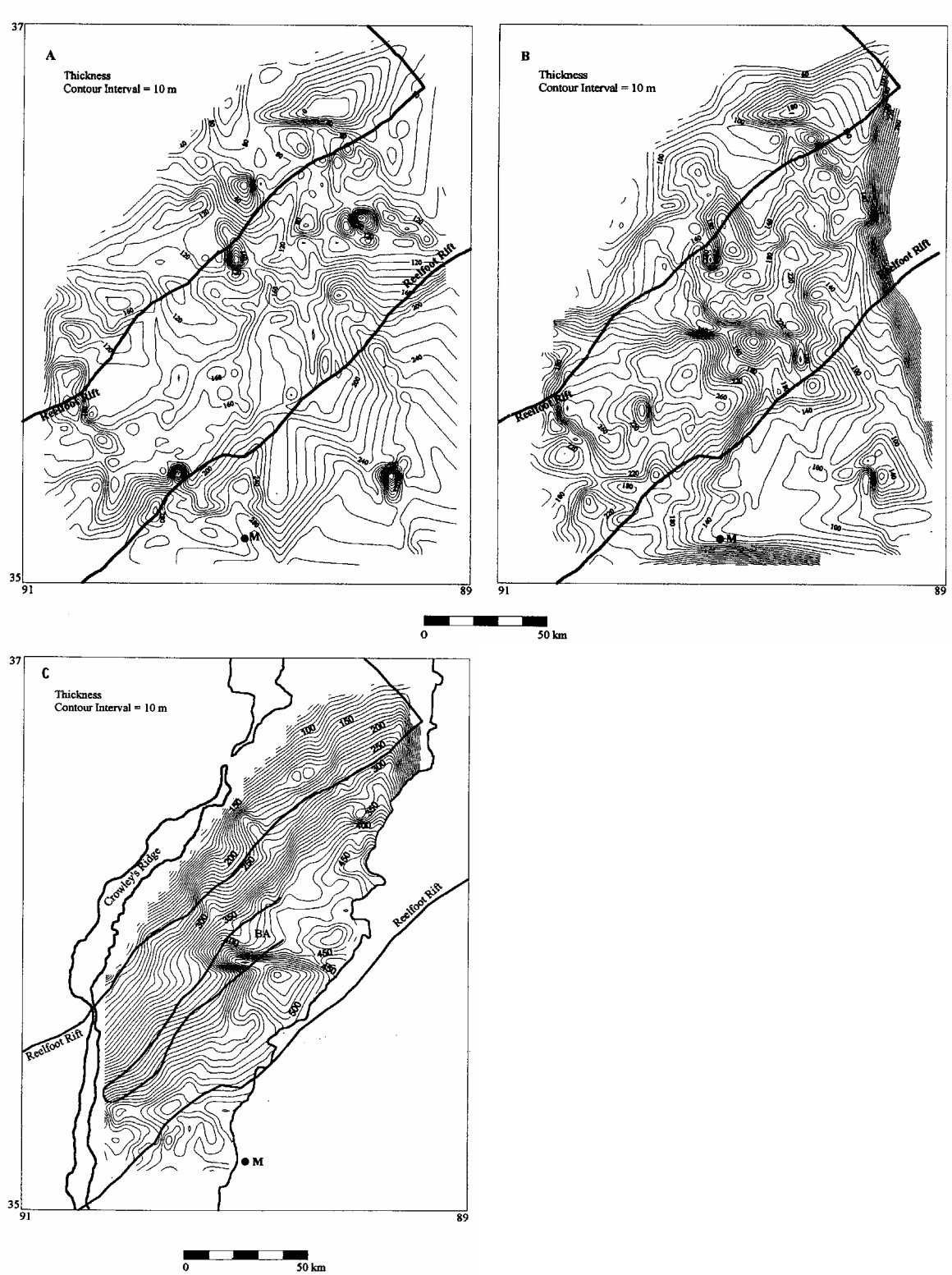

Figure 7. Isopach maps of the Upper Cretaceous (A), Paleocene Midway Group (B), and the Eocene section (C) that includes the Wilcox Group, Claiborne Group, and Jackson Formation (20). M = Memphis.

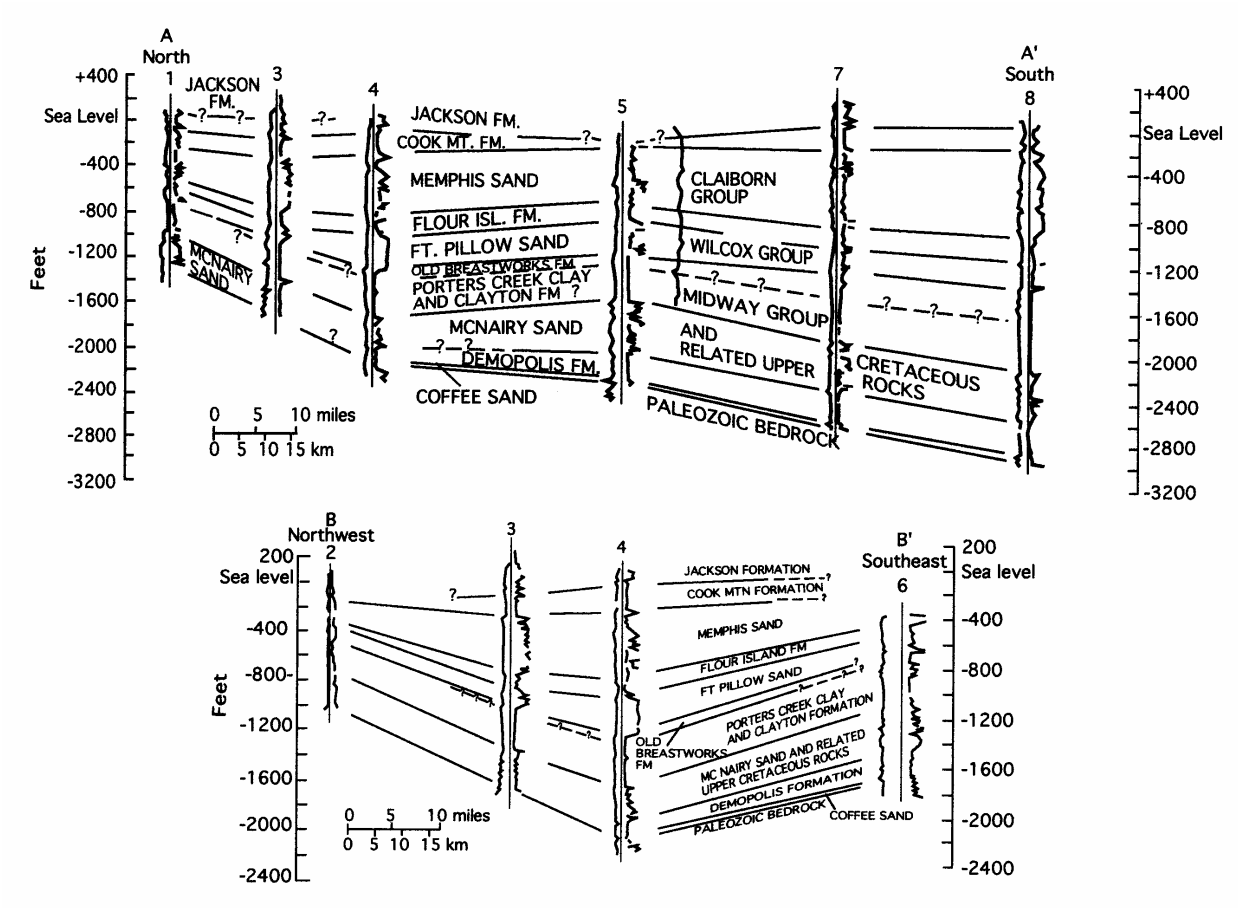

Figure 8. Stratigraphic cross sections A-A' and B-B' in the northern Mississippi embayment (22). The cross sections are located on Figure 1. The well names are 1 = #1 E. Phillips, 2 = #1 Oliver, 3 = New Madrid test well 1-X, 4 = #1 J.E. Vaughn, 5 = #1 T.A. Lee, 6 = #1 Vance Holt, 7 = Fort Pillow test well, and 8 = USGS SH:TL8.

interbedded with thin carbonaceous clays (23). This formation is approximately 32 m thick beneath Shelby County but thins northward and is not present in the New Madrid test well (Fig. 1, well #3) (22,24). Overlying the Coffee Formation in the southern part of the cross section is the Demopolis Formation (25). The Demopolis Formation is a calcareous marine clay that thins northward. Beneath Shelby County the clay is 140 m thick, but it is not present in the New Madrid test well. Overlying the Demopolis Formation is the McNairy Sand. This unit is a 130 m thick calcareous marine sand beneath Shelby County, but it grades to a fluvial/deltaic sand northward where it thins to 95 m beneath New Madrid.

Paleocene - Miocene Depositional History

An unconformity separates the Late Cretaceous McNairy Sand and overlying Paleocene Midway Group. This unconformity marks the Late Cretaceous regression, subaerial exposure of the Late Cretaceous sediments, and Paleocene transgression of the Mississippi embayment sea. The Midway Group is a marine clay that thins from 160 m in Shelby County to 100 m beneath New Madrid. Unconformably overlying the Midway Group is the Paleocene to Eocene Wilcox Group. In ascending order, the Wilcox is subdivided into the Old Breastworks Formation, the Fort Pillow Sand, and the Flour Island Formation. The Old Breastworks Formation is a 95 m thick clayey silt beneath Shelby County (19) that grades to a silty clay in the New Madrid test well (24) and pinches out northward beneath the town of New Madrid. The Fort Pillow Sand is a 64 m thick marine sand at Shelby County that thins and grades to a fluvial/deltaic sand northward where it is 32 m thick beneath New Madrid. Overlying the Fort Pillow Sand is the Flour Island Formation, which consists of alternating beds of silt, clay, and sand. This unit also is more terrestrial from south to north and thins northward from 80 m to 31 m. An unconformity marks the top of the Wilcox Group. The overlying middle Eocene Claiborne Group marks a marine transgression and is subdivided in ascending order into the Memphis Sand, the Cook Mountain Formation, and the Cockfield Formation. In this cross section (Fig. 8); however, the Cook Mountain and Cockfield formations are combined and labeled as Cook Mountain Formation. The Memphis Sand is a fluvial/deltaic sand that is 223 m thick beneath Shelby County and thins northward to 110 m thick beneath New Madrid. The overlying Cook Mountain Formation is a clay and silt fluvial/deltaic unit with minor sand lenses and lignite beds (24). Cockfield Formation sediments consist of fluvial/deltaic silt and clay interbedded with sand and lignite beds. The combined thickness of the Cook Mountain and Cockfield formations is 64 m in Shelby County, thinning to 30 m in Lauderdale County, Tennessee (well #5 of Fig. 8), and thickening to 48 m beneath New Madrid. The Eocene to Oligocene Jackson Formation (26) is a fluvial/deltaic silty sand interbedded with clayey silt and lignite that is 16 m thick in Shelby County and 41 m thick beneath New Madrid. Jackson Formation thickness is quite variable because its upper contact is an unconformity overlain by Quaternary Mississippi River alluvium within the valley and by Pliocene-Pleistocene Lafayette Formation (Upland Gravel) on the bluffs east of the Mississippi River (27). With the exception of Miocene gravels (28,29), there are no Oligocene or Miocene sediments above the Jackson Formation in the NME. Thus, it appears that the NME has been above sea level since Oligocene Jackson Formation time.

Pliocene - Quaternary Depositional History

The surface and near-surface stratigraphy is different east and west of the Mississippi River in the NME and changes along the line of section between the #1 J. E. Vaughn and #1 T. A. Lee wells (Fig. 8). West of the Mississippi Valley bluff line, the surface stratigraphy consists of Mississippi River Pleistocene (terraces) and Holocene alluvium. East of the bluff line the near-surface stratigraphy consists of the Lafayette Formation (Upland Gravel) and the overlying Pleistocene loess.

The Mississippi River sediments, which are approximately 50 m thick, consist of a basal sandy gravel overlain by sands and capped by silts and clays (Saucier, 1994). These flood plain sediments are below the Lafayette Formation and inset 64 m into the Jackson Formation. Thus, approximately 14 m of Jackson Formation is exposed in the base of the Mississippi River Valley bluffs (30).

On the bluffs and on Crowley's Ridge (Fig. 1) the Lafayette Formation locally overlies the Jackson Formation (31,27). Lafayette Formation fluvial sands and gravels vary in thickness because both the upper and lower contacts are erosional; an average thickness is 16 m. Overlying the Lafayette Formation on the Mississippi Valley bluffs is Pleistocene loess (32,33). This loess consists of at least three wind-blown silt units with a cumulative thickness as much as 34 m immediately east of the Mississippi River that thins eastward. An average thickness for the loess along the bluff line is 17 m.

Post-Paleozoic Structure of the Northern Mississippi Embayment

Seismic reflection surveys provide information as to the timing, style, and magnitude of post-Paleozoic fault movement within the NME (34,35,36,37,38,39,40,41,42,43,44,45,46,47, 48,49,50). A seismic reflection study of Crowley's Ridge and vicinity near Jonesboro (Fig. 9) imaged a west-bounding fault of the Reelfoot rift (51). On this seismic line there is no indication of Cretaceous faulting; however, the Midway Group thickens across the fault and thus indicates Paleocene normal fault displacement. This same fault and other faults that bound Crowley's Ridge also have minor Paleocene-Eocene normal displacement as revealed by thickening of the Wilcox Group. Minor post-Wilcox normal faults and post-Claiborne reverse faults are evident on many of the Crowley's Ridge reflection lines. The Crittenden County fault (44) and the Cottonwood Grove fault (35,45) (Fig. 9) show middle to late Eocene Claiborne compressional deformation. The Reelfoot fault (Fig. 9) is a southwest-dipping reverse fault along the eastern margin of the Lake County uplift. This fault has been reactivated a number of times since the Paleozoic and most recently in 1812 (38,52). Bedrock exposures in the Benton Hills of southeastern Missouri reveal strike slip faulting (29) along the Commerce fault (Fig. 9) that has been episodic throughout the Cenozoic with from 4 to 6 faulting events within the late Quaternary (53).

To better understand the post-Paleozoic structure of the NME in a regional perspective, subsurface data were collected (20) and structure contour maps were constructed of the tops of the Paleozoic section, Late Cretaceous section, Paleocene Midway Group, and Eocene section. Similarly, isopach maps were made of the Late Cretaceous section, Midway Group, and Eocene section to determine when the deformation occurred and also to illustrate the thicknesses and distributions of these units. We shall ignore the isolated anomalies associated with individual

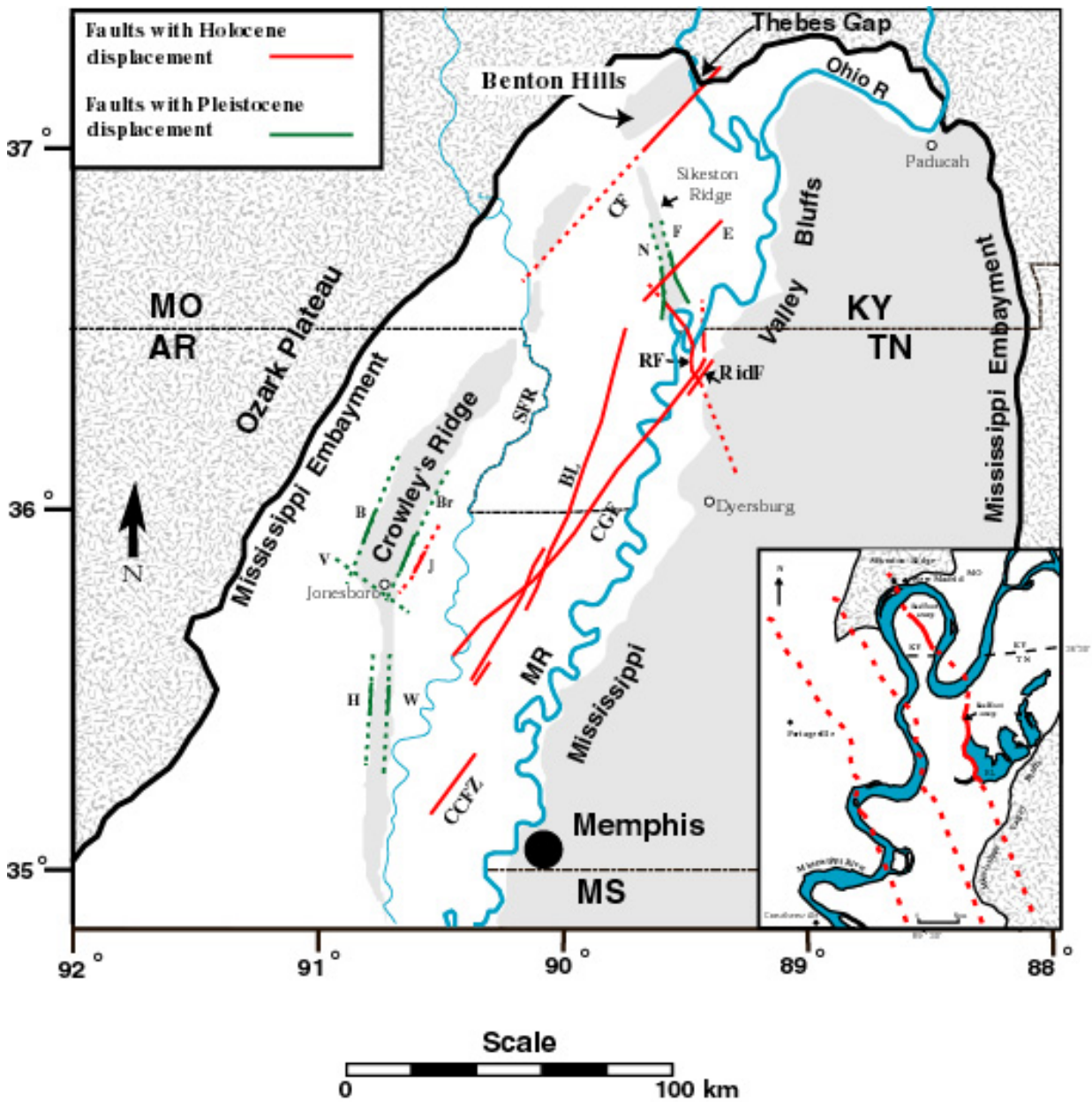

Figure 9. Quaternary faults in the New Madrid seismic zone and vicinity. Faults discussed in text are RF = Reelfoot fault, RidF = Ridgely fault, CGF = Cottonwood Grove Fault, BL = Bootheel Lineament, CCFZ = Crittendend County fault, J = Jonesboro fault, CF = Commerce fault. Inset is Reelfoot fault and its back thrusts near New Madrid, MO and Reelfoot Lake, TN. MR = Mississippi River

wells and focus on the regional features of the maps.

Structure Contour Maps

The structure contour map of the top of the Paleozoic strata illustrates that the NME is a southwest-plunging trough (Fig. 3) (54). However, this trough is very gentle. Specifically, the eastern limb of the NME trough dips 0.3^0 west, the western limb dips 0.5^0 southeast, and the trough plunges 0.1^0 south. The Paleozoic-Late Cretaceous unconformity and overlying sediments within the NME are essentially flat lying.

The Paleozoic and Cretaceous structure contour maps are nearly identical (Figs. 3 and 4). The Midway structure contour map is very similar to the underlying surfaces; differences probably are because fewer seismic reflection data are available for the Midway map (Fig. 5). East-west cross sections (not shown here) across the southern map area at Memphis and across the northern map area at the Lake County uplift reveal that total structural relief on the Paleozoic, Late Cretaceous, and Midway Group is approximately 540 m, 570 m, and 400 m respectively. The Figures 3-5 structure contour maps do, however, reveal a subtle, 50-km-wide "trench" within the NME trough. On the Paleozoic surface, the maximum depth of the trench is approximately 100 m both at Memphis and at the southern margin of the Lake County uplift (Fig. 3). On both the Cretaceous and Midway Group surfaces, the maximum depth of the trench is approximately 50 m both at Memphis and at the southern margin of the Lake County uplift (Figs. 4 and 5).

Figure 6 is a structure contour map of the Eocene/Quaternary unconformity (55). In general, there is good agreement between areas of known or suspected 1811-1812 coseismic uplift and subsidence and respective highs and lows (hachured) on the unconformity surface. The Reelfoot Lake basin east of the Lake County uplift (LCU) is evident on the unconformity surface as a structural low. The LCU and Blytheville Arch (BA) are structural highs on the unconformity, with the LCU having as much as 30 m of relief. Furthermore, the structure contour map suggests the LCU may extend southeastward beyond Ridgely Ridge to the edge of the bluffs. We believe that uplift on the hanging wall of the Reelfoot fault has caused this high on the unconformity. This apparent southeastern continuation of the LCU supports the interpretation of Van Arsdale et al. (56) that hanging wall uplift on the Reelfoot fault continues at least 32 km southeast of Reelfoot Lake.

A wide, sinuous low on the unconformity exists northwest of the Blytheville arch (Fig. 6). This low begins on the west side of the LCU and trends south. Near the southern termination of the LCU, the low turns more southwesterly. The southwestern portion of the low is beneath the sunklands of northeastern Arkansas. Uplift of the Blytheville arch and concurrent subsidence on the arch's northwest flank has been proposed as an explanation for the formation of these sunklands (49). The sinuous low could be a former course of an ancestral Mississippi River, but a tectonic origin is preferred because; 1) it underlies the sunklands that are interpreted to have experienced several episodes of subsidence (57), 2) the low terminates against Crowley's Ridge, which is composed of Eocene strata capped by Lafayette Formation and loess, 3) it does not follow any Quaternary Mississippi River courses as mapped by Saucier (58), and 4) the low underlies four geomorphic surfaces of different ages (27).

The unconformity surface has a series of small circular lows, the largest of which is coincident with a major deflection in the course of the Mississippi River. The origin of the

circular lows and apparent deflection of the Mississippi River is unknown although the circular lows may be due to isolated scours along the Mississippi River or artifacts of the contouring.

The Crittenden County fault (Fig. 9) is a down-to-the-east reverse fault (44) that has Quaternary displacement (46). The unconformity displays significant lows east and west of the fault with relief up to 25 m (Fig. 6). We believe that 25 m of relief is probably too much to attribute solely to late Wisconsin through Holocene uplift on the Crittenden County fault and therefore suspect that scour by the Mississippi River east and west of the fault has contributed to the relief on the unconformity.

Except for the Reelfoot and Crittenden County faults, subsurface faults within the NME (34,35,38,50,49,51,52) are not evident on our structure contour maps. This is probably because most NME faults have too little vertical displacement to be evident in maps of this scale. However, there are a number of flexures in the contour lines that may represent northwest-trending faults (Figs. 3 and 4). It is also possible that the borders of the trench are fault controlled. Most notable are the closely spaced contour lines near Memphis that may reflect a down-to-the-west fault (Fig. 3) (59,20).

Isopach Maps

Isopach maps of the Upper Cretaceous section, the Midway Group, and the Eocene section illustrate the thicknesses of these units within the NME (Fig. 7). The Upper Cretaceous section thickens southeasterly (1). Near Memphis the Upper Cretaceous section is thick within the trench mapped on the surface of the Paleozoic; however, farther north the contours indicate that the section thickens to the southeast, nearly at right angles to the trench.

The Midway Group is thickest in the central part of the map within the boundaries of the Reelfoot rift. There is no indication of Midway thickening over the trench mapped at the top of the Late Cretaceous section.

The Eocene section isopach only includes the area between Crowley's Ridge and the bluffs and thus only covers the central part of the other isopach maps. However, it is apparent that the Eocene section thickens from west to east. The thickest part of the Eocene section overlies the trench on the surface of the underlying Midway Group.

Discussion and Conclusions

The structure contour map of the top of the Paleozoic displays a southerly plunging trough within the NME (Fig. 3). Unlike the vertically exaggerated bowl-shaped trough that is commonly portrayed, the NME unconformity and overlying Upper Cretaceous and Cenozoic sediments are essentially flat. Subtle features within the structure contour and isopach maps do, however, reveal information on the history and tectonics of the NME.

The Upper Cretaceous isopach portrays the strata uniformly thickening to the southeast across the Reelfoot rift boundaries and thus there is no indication that the Reelfoot rift influenced Late Cretaceous sedimentation (Fig. 7A). The Paleocene Midway Group is thicker within the boundaries of the Reelfoot rift; and, therefore, minor rift reactivation appears to have occurred during Paleocene time (Fig. 7B). The Eocene isopach does not cover the entire Reelfoot rift; however, the western rift margin does not appear to have affected Eocene deposition (Fig. 7C). Thus, we conclude that within the NME of this 2^0 study area, the seismic reflection studies and

our maps indicate; 1) no Late Cretaceous vertical faulting, 2) extensional faulting occurred during the Paleocene and lower Eocene, 3) extensional and compressional faulting occurred from middle to late Eocene, and 4) compressional faulting has and continues to occur during the Quaternary. Because the NME has apparently been subaerially exposed since deposition of the Eocene-Oligocene Jackson Formation it is possible that the NME has been under compression since Jackson Formation time.

The structure contour maps reveal a subtle depression that we have called a trench at the tops of the Paleozoic, Upper Cretaceous, and Midway Group along the axis of the NME. This trench has very similar size, depth, and location on all three surfaces. Because each of these surfaces is an unconformity, it is possible that these trenches are ancestral courses of the Mississippi River. However, we believe that the geometric similarity and superposition of the three trenches suggests a common structural origin. There is no evidence for the trench in the Upper Cretaceous or Midway Group isopachs, suggesting that the trench is younger than Paleocene. The Eocene section thickens easterly and is thickest atop the western side of the underlying trench. Thus, it appears that the trench that defines the axis of the NME, formed in Eocene time. It also appears that the trench is unrelated to the Reelfoot rift because the trench crosses the southeastern border of the rift (Figs. 3-5).

The Blytheville arch/Lake County uplift is coincident with the western side of the trench for much of its length (Fig. 3). Relative uplift of the Blytheville arch/Lake County uplift appears to have formed the western margin of the trench in Eocene time. On the basis of distribution of Quaternary Mississippi River sediments, we believe this relative uplift has also occurred during the Quaternary. Mississippi River terraces descend topographically and are younger eastward from Crowley's Ridge (58). Thus, the Mississippi River has shifted eastward during the Quaternary to its present Holocene position (51), atop the western half of the trench. The New Madrid seismic zone is coincident with the Blytheville arch/Lake County uplift, therefore, displacement across the western margin of the trench, albeit minor, may be localizing earthquakes of the New Madrid seismic zone and controlling the Holocene position of the Mississippi River.

Apparently contradicting the observation that a trench may be subsiding beneath the NME during Quaternary time, are both the post-Jackson Formation subaerial emergence history and the fact that the Quaternary Mississippi River alluvium is incised through the Lafayette Formation (Upland Gravel) into the Eocene section. The Mississippi River in the NME has incised approximately 80 m since deposition of the Pliocene-Pleistocene Lafayette Formation.

In order to reconcile this apparent contradiction, we propose that the entire NME is under compression and undergoing differential uplift. We also believe that the NME has been rising during the Quaternary (8), but the trench has lagged behind. This regional differential uplift interpretation is consistent with the observation that Crowley's Ridge appears to have Wisconsin uplift (51) and that Holocene uplift is occurring on the Blytheville arch/Lake County uplift of the New Madrid seismic zone (35,49).

Areas that have experienced Holocene uplift include the Lake County uplift, Blytheville arch, and the Crittenden County fault. Areas that have experienced Holocene subsidence include Reelfoot Lake, historical Lake Obion, the Sunklands of northeast Arkansas, and perhaps areas east and west of the Crittenden County fault (55). All of these areas are clearly visible as areas of apparent uplift and subsidence on the unconformity that separates the Eocene and Quaternary deposits (Fig. 6). Thus, we believe that Figure 6 is primarily a structure contour map illustrating

structural deformation that has occurred during Late Wisconsin through Holocene time. In addition, Figure 6 is a strain field map that provides constraints on kinematic modelling of NMSZ faulting (60,61) while illustrating the pattern of deformation that should be expected in future great New Madrid earthquakes.

The post-Paleozoic NME sedimentary package increases from 477 m thick at New Madrid to 987 m at Shelby County. These sediments are both terrestrial and marine but their compositions are quite uniform and there appears to be little lithification. Thus, we expect that the seismic velocities within and among these mapped units are very similar throughout the NME as is indicated by the interval velocities used in this study. Lithologic descriptions of the New Madrid and Fort Pillow test wells along the line of section from New Madrid, Missouri, to Shelby County, Tennessee, describe sands, silts, and clays. These lithologic logs do not identify any cementation and thus suggest unconsolidated clastic sediment. However, Jackson Formation siltstones are exposed in the Mississippi River bluffs of western Tennessee. These siltstones are locally quite indurated, and so we include these field observations to acknowledge that we do not really know the degree of lithification within the Late Cretaceous and Tertiary section of the NME. As in the uncertainty about lithification, we must add the caveat that seismic reflection profiles in the NME reveal acoustical impedance (strong reflections) at the unconformity surfaces at the tops of the Paleozoic, Upper Cretaceous, Midway Group, Wilcox Formation, and Eocene section (35,44,62,51,52) that may influence seismic wave transmission.

References

1. Stearns, R.G. (1957). Cretaceous, Paleocene, and Lower Eocene geologic history of the northern Mississippi embayment, *Geol. Soc. Am. Bull.* **68**, 1077-1100.

2. Pryor, W.A. (1960). Cretaceous sedimentation in upper Mississippi embayment, *Am. Assoc. Pet. Geol. Bull.* **44**, 1473-1504.

3. Burke, K. and Dewey, J.F. (1973). Plume-generated triple junctions: key indicators in applying plate tectonics to old rocks, *J. of Geol*. **81**, 406-433.

4. Ervin, C.P. and McGinnis, L.D. (1975). Reelfoot rift-Reactivated precursor to the Mississippi Embayment, *Geol. Soc. Am. Bull.* **86**, 1287-1295.

5. Kane, M.F., Hildenbrand, T.G., and Hendricks, J.D. (1981). Model for the tectonic evolution of the Mississippi embayment and its contemporary seismicity, *Geology* **9**, 563-568.

6. Braile, L.W., Keller, G.R., Hinze, W.J., and Lidiak, E.G. (1986). An ancient rift complex and its relation to contemporary seismicity in the New Madrid seismic zone, *Tectonics* **1**, 225-237.

7. Cox, R.T., and Van Arsdale, R.B. (1997). Hotspot origin of the Mississippi embayment and its possible impact on contemporary seismicity, *Eng. Geol.* **46**, 5-12.

8. Fisk, H.N. (1944). Geological investigation of the alluvial valley of the lower Mississippi River, *US Army Corps of Engineers, Mississippi River Comm., Vicksburg, MS*, 78.

9. Caplan, W.M. (1954). Subsurface geology and related oil and gas possibilities of northeastern Arkansas, *Ark. Res. and Development Com. Div. of Geol. Bull.* **20**, 124.

10. Murray, G.E. (1961). Geology of the Atlantic and Gulf Coastal Province of North America, *Harper & Brothers, Publishers, New York*, 692.

11. Stearns, R.G. and Marcher, M.V. (1962). Late Cretaceous and subsequent structural development of the northern Mississippi embayment area, *Geol. Soc. Am. Bull.* **73**, 1387-1394.

12. Marcher, M.V. and Stearns, R.G. (1962). Tuscaloosa Formation in Tennessee, *Geol. Soc. Am. Bull.* **73**,1365-1386.

13. Boswell, E.H., Moore, G.K., MacCary, L.M., and others (1965). Cretaceous Aquifers in the Mississippi Embayment, *US Geol. Survey Prof. Paper* **448**-C, 37.

14. Petersen, J.C., Broom, M.E., and Bush, W.V. (1985). Geohydrologic units of the Gulf Coastal Plain in Arkansas, *US Geol. Surv. Water-Resources Inves. Report* **85-4116**, 20.

15. Brahana, J.V., and Mesko, T.O. (1988). Hydrogeological and preliminary assessment of regional flow in the upper Cretaceous and adjacent aquifers in the northern Mississippi embayment, *US Geol. Survey Water Res. Invest. Report* **87-4000**, 65.

16. Galloway, W.E., Bedout, D.G., Fisher, W.L., Dunlap, J.B., Cabrera-Castro, R., Lugo-Rivera, J.E., and Scott, T.M. (1991). The Geology of North America Vol. J, The Gulf of Mexico Basin, *The Geol. Soc. of Am*., 245-324.

17. Sharp, J.M., Kreitler, C.W., and Lesser, J. (1991). The Geology of North America Vol. J, The Gulf of Mexico Basin, *The Geol. Soc. of Am.*, 529-543.

18. Sohl, N.F., Martinez, E.R., Salmeron-Urena, P., and Soto-Jaramillo, F. (1991). The Geology of North America Vol. J., The Gulf of Mexico Basin, *The Geol. Soc. of Am.*, 205-244.

19. Hosman, R.L. (1996). Regional stratigraphy and subsurface geology of Cenozoic deposits, Gulf Coastal Plain, south-central United States, *US Geol. Surv. Prof. Paper* **1416-G**, 35.

20. Mihills, R.K. (1998). A structural analysis of the New Madrid seismic zone from structure contour maps and a three-dimensional model, *MS Thesis, University of Memphis, Memphis, TN*, 82.

21. Kekler, D. (1995). Surfer for Windows, version 6 user's guide, *Golden Software, Inc., second ed.*

22. Crone, A.J. (1981). Sample description and stratigraphic correlation of the New Madrid test well-1-X, New Madrid County, Missouri, *U.S. Geol. Surv. Open-File Rep.* **81-426**, 26.

23. Russell, E.E., Keady, D.M., Mancini, E.A., and Smith, C.E. (1982). Upper Cretaceous in the lower Mississippi embayment of Tennessee and Mississippi: lithostratigraphy and biostratigraphy, *Field trip guidebook for the 1982 annual meeting of the Geol. Soc. Am., New Orleans, LA*, 40.

24. Fredericksen, N.O., Bybell, L.M., Christopher, R.A., Crone, A.J., Edwards, L.E., Gibson, T.G., Hazel, J.E., Repetski, J.E., Russ, D.P., Smith, C.C., and Ward, L.W. (1982). Biostratigraphy and paleoecology of Lower Paleozoic, Upper Cretaceous, and Lower Tertiary rocks in U.S. Geological Survey New Madrid test wells, southeastern Missouri, *Tulane Studies in Geology and Paleontology* **17**, 23-45.

25. Moore, G.K. and Brown, D.L. (1969). Stratigraphy of the Fort Pillow test well, Lauderdale County, Tennessee, *Tenn. Dept. of Conserv., Div. of Geol., Report of Investigations* **26**.

26. Nelson, J.W. (1998). Bedrock geology of the Paducah 1^0x2^0 CUSMAP quadrangle, Illinois, Indiana, Kentucky, and Missouri, *US Geol. Surv. Bull.* **2150-B**, 36.

27. Autin, W.J., Burns, S.F., Miller, B.J., Saucier, R.T., and Snead, J.I. (1991). Quaternary geology of the Lower Mississippi Valley, in Quaternary nonglacial geology: conterminous U.S., R.B. Morrison (Editor), *GSA, Boulder, CO*, 547-582.

28. Olive, W.W. (1980). Geologic maps of the Jackson Purchase region, Kentucky, *US Geol. Surv. Misc. Invest. series*, 1:250,000 scale.

29. Harrison, R.W. and Schultz, A. (1994). Strike-slip faulting at Thebes Gap, Missouri and Illinois: implications for New Madrid tectonism, *Tectonics* **13**, 246-257.

30. Hardeman, W.D. (1966). Geologic map of Tennessee west sheet, *State of Tenn. Dept. of Conserv. Div. of Geol.*, 1:250,000 scale.

31. Potter, P.E. (1955). The petrology and origin of the Lafayette gravel, *J. Geol.* **63(1), 1-38**, 115-132.

32. Rutledge, E.M., Guccione, M.J., Markewich, H.W., Wysocki. D.A., and Ward, L.B. (1996). Loess stratigraphy of the lower Mississippi valley, *Eng. Geol.* **45**, 167-183.

33. Rodbell, D.T., Forman, S.L., Pierson, J., and Lynn, W.C. (1997). Stratigraphy and chronology of Mississippi Valley loess in western Tennessee, *Geol. Soc. Am. Bull.* **109**, 1134-1148.

34. Zoback, M.D. (1979). Recurrent faulting in the vicinity of Reelfoot Lake, northwestern Tennessee, *Geol. Soc. Am. Bull.* **Part 1, 90**, 1019-1024.

35. Hamilton, R.M. and Zoback, M.D. (1982). Tectonic features of the New Madrid seismic zone from seismic-reflection profiles, in Investigations of the New Madrid, Missouri, earthquake

region, F. A. McKeown and L. C. Pakiser (Editors), *U S Geol. Surv. Prof. Paper* **1236**, 55-82.

36. Shedlock, K.M. and Harding, S.T. (1982). Mississippi River seismic survey, *Geophy. Res. Lett.* **9**, 1275-1278.

37. Howe, J.R. (1985). Tectonics, sedimentation, and hydrocarbon potential of the Reelfoot aulacogen, *MS Thesis, University of Oklahoma, Norman, OK*, 109.

38. Sexton, J.L., and Jones, P.B. (1986). Evidence for recurrent faulting in the New Madrid seismic zone from Mini-Sosie high-resolution reflection data, *Geophysics* **51**, 1760-1788.

39. Sexton, J.L. and Jones, P.B. (1988). Mini-Sosie high-resolution reflection survey of the Cottonwood Grove fault in northwestern Tennessee, *Seism. Soc. Am. Bull.* **78**, 838-854.

40. Nelson, K.D. and Zhang, J. (1991). A COCORP deep reflection profile across the buried Reelfoot rift, south-central United States, *Tectonophysics* **197**, 271-293.

41. Crone, A.J. (1992). Structural relations and earthquake hazards of the Crittenden County fault zone, northeastern Arkansas, *Seism. Res. Lett.* **63**, 249-262.

42. Schweig, E.S., Fan, Shen, Kanter, L.R., Luzietti, E.A., Van Arsdale, R.B., Shedlock, K.M., and King, K.W. (1992). Shallow seismic reflection survey of the Bootheel lineament area, southeastern Missouri, *Seism. Res. Lett.* **63**, 285-295.

43. Sexton, J.L., Henson, H., Dial, P., and Shedlock, K. (1992). Mini-Sosie high resolution seismic reflection profiles along the Bootheel Lineament in the New Madrid seismic zone, *Seism. Res. Lett.* **63**, 297-307.

44. Luzietti, E.A., Kanter, L.R., Shedlock K.M., Schweig, E.S., and Van Arsdale, R.B. (1995). Shallow deformation along the Crittenden County fault zone near the southeastern margin of the Reelfoot rift, northeast Arkansas, in Investigations of the New Madrid seismic zone, K.M. Shedlock and A.C. Johnston (Editors), *US Geol. Surv. Prof. Paper* **1538-J**, 23.

45. Stephenson, W.J., Shedlock, K.M., and Odum, J.K. (1995). Characterization of the Cottonwood Grove and Ridgely faults near Reelfoot Lake, Tennessee, from high-resolution seismic reflection data, *US Geol. Surv. Prof. Paper* **1538-I**, 1-10.

46. Williams, R.A., Luzietti, E.A., and Carver, D.L. (1995). High-resolution seismic imaging of Quaternary faulting on the Crittenden County fault zone, New Madrid seismic zone, northeastern Arkansas, *Seism. Res. Lett.* **66**, 42-57.

47. Woolery, E.W., Wang, Z., Street, R.L., and Harris, J.B. (1996). A P-and SH-wave seismic reflection investigation of the Kentucky Bend scarp in the New Madrid seismic zone, *Seism. Res. Lett.* **67**, 67-74.

48. Odum, J.K., Stephenson, W.J., Shedlock, K.M., and Pratt, T.L. (1998). Near surface structural model for deformation associated with the February 7, 1812, New Madrid, Missouri, earthquake, *Geol. Soc. of Am. Bull.* **46**, 149-162.

49. Van Arsdale, R.B. (1998). Seismic hazards of the upper Mississippi embayment, *US Army Corps of Engineers Waterways Experiment Station Contract Report* **GL-98-1**, 55.

50. Purser, J.L, and Van Arsdale, R.B. (1998). Structure of the Lake County uplift: New Madrid seismic zone, *Seism. Soc. Am. Bull.* **88**, 1204-1211.

51. Van Arsdale, R.B., Williams, R.A., Schweig, E.S., Shedlock, E.S., Odum, J.K., and King, K.W. (1995). The origin of Crowley's Ridge, northeastern Arkansas: erosional remnant or tectonic uplift?, *Seism. Soc. Am. Bull.* **85**, 963-985.

52. Van Arsdale, R.B., Purser, J., Stephenson, W., and Odum J. (1998). Faulting along the southern margin of Reelfoot Lake, Tennessee, *Seism. Soc. Am. Bull.* **88**, 131-139.

53. Harrison, R.W., Palmer, J.R., Hoffman, D., Vaughn, J.D., Forman, S.L., McGeehin, J., and Frederiksen, N.O. (1997). Profiles and documentation of fault-exploration trenches in the English Hill area, Scott City 7.5-minute quadrangle, Missouri, *US Geol. Surv. Open-File Report* **97-474**, 96.

54. Wheeler, R.L., Rhea, S., and Dart, R.L. (1994). Map showing structure of the Mississippi Valley graben in the vicinity of New Madrid, Missouri, *USGS Miscellaneous Field Studies Map* **MF-2264-D**.

55. Mihills, R.K. and Van Arsdale, R.B., 1999, Late Wisconsin to Holocene deformation in the New Madrid seismic zone, *Seism. Soc. Am. Bull.* **89**, 1019-1024.

56. Van Arsdale, R.B., Cox, R.T., Johnston, A.C., Stephenson, W.J., and Odum, J.K. (1999). Southeastern extension of the Reelfoot scarp, *Seism. Res. Lett.*,**70**, 352-363.

57. Guccione, M.J., Van Arsdale, R.B., and Hehr, L.H., 2000, Origin and age of the Manila high and associated Big Lake "sunklands" in the new Madrid seismic zone, northeastern Arkansas, *Geol. Soc. Am. Bull.* **112**, 579-590.

58. Saucier, R.T. (1994). Geomorphology and Quaternary geologic history of the lower Mississippi Valley, *U.S. Army Corps of Engineers Waterways Experiment Station*, 364.

59. Johnson, P.R., Zietz, I., and Thomas, W.A. (1994). Possible Neoproterozoic-early Paleozoic grabens in Mississippi, Alabama and Tennessee, *Geology* **22**, 11-14.

60. Gomberg, J. (1993). Tectonic deformation in the New Madrid seismic zone: inferences from map view and cross-sectional boundary element models, *J. Geophy. Res*., **98**, 6639-6664.

61. Gomberg, J. and Ellis, M.A. (1994). Topography and tectonics of the central New Madrid seismic zone: results of numerical experiments using a three-dimensional boundary element program, *J. Geophy. Res*., **99**, 299-310.

62. Odum, J.K., Luzietti, E.A., Stephenson, W.J., Shedlock, K.M., and Michael, J.A. (1995). High-resolution, shallow, seismic reflection surveys of the northwest Reelfoot rift boundary near Marston, Missouri, *US Geol. Surv. Prof. Paper* **1538-P**, 18.

Part 2: Forward Modeling of the Rupture Scenario of the 1811 - 1812 Earthquakes.

Abstract

We have derived a rupture scenario for the great New Madrid earthquakes of 1811-1812 through a series of numerical experiments that integrate extensive historical and geomorphic accounts of changes of topography. The rupture scenario that most consistently explains all observations, that explains subsequent moderate earthquakes in the New Madrid region, that is capable of being generated by a single uniform stress field, and that is most consistent with remote driving forces from the mid-Atlantic ridge involves a left-stepping, right-lateral strike-slip system, part of which lies along the Bootheel lineament, which is currently aseismic.

Introduction

A major obstacle to understanding seismicity and seismic hazard in stable continental regions is that large earthquakes in these areas are rare, making it difficult to make statistically valid statements about what are "typical" characteristics of these events. One way to increase the knowledge base of these intraplate earthquakes is to supplement it with the historical and geological record of pre-instrumental earthquakes. In this report we integrate the historical and geomorphic record to obtain the most likely rupture scenario for the New Madrid earthquake sequence, three of the largest earthquakes in stable continental regions in historical times.

These moment-magnitude **M**~8 earthquakes (1) occurred in the winter of 1811-1812 in the central Mississippi River Valley of the United States. They are thought to be related to the reactivation of structures within the Reelfoot rift, a failed plate boundary of late Precambrian age. Much of the current seismicity is aligned along the rift axis and the northwestern margin of the rift, although the very active central zone is at a high angle to it.

The last five years have seen a rapid increase in our understanding of deformation in the New Madrid region. Most significantly, we now recognize that earthquakes large enough to cause liquefaction similar in scale to that generated by the sequence in 1811-1812 have occurred at least three times in the last 2000 years (2). Analysis of horizontal ground deformation using the global positioning satellite system has failed to yield an unambiguous estimate of active shear strain rates, because insufficient time has elapsed for the signal to rise above the background noise (3), although earlier analyses are consistent with a recurrence interval of less than 1,000 years and as low as ~500 years (4).

Despite the apparent high rate of occurrence, there is relatively little finite deformation in

the subsurface, which we attribute to the young age of the active deformation (4). More particularly, little direct evidence exists of surface ruptures within a 650,000 square km area that was otherwise extensively liquefied. Earthquakes of the magnitude of the 1811-1812 sequence (**M** 8) require rupturing faults with a length of ~175 to ~350 km if average displacements scale as $u = 3.9 \times 10^{-7} M_o^{1/3}$ (5) and for rupture depths of 40 km to 20 km, respectively. Average displacements are more difficult to predict, as there is uncertainty about which length-dimension of the rupture is the appropriate scaling length. Using a value of L ranging from 94 km (the equivalent diameter of rupture area derived from the scaling relation between u and M_o cited above) to 350 km gives a range of average displacement from ~4 to ~15 m. Alternatively, using the scaling proposed recently by McGarr and Fletcher (5) in which $u_{max} = 10^{-5.83}.M_o^{1/3}$, yields a maximum displacement of ~10 m to ~15 m for a **M** of 7.7 and 8.0, respectively. These figures illustrate the uncertainty behind estimates of displacement associated with the New Madrid earthquakes, and we have no information about probability density functions relevant to these uncertainties. The only direct evidence of surface rupture is limited, however, to the 32 km-long Reelfoot scarp in the central seismic zone (6).

Considerable indirect evidence exists, however, for the locations of 1811-1812 source faults and for one or more of the larger (**M**~7) aftershocks. The bulk of this evidence is in the form of subtle changes of topography that occurred during and immediately after the sequence of large earthquakes, but also includes the prominent Bootheel lineament (7) and historical evidence. We use a three-dimensional boundary-element algorithm (8) to calculate the spatial distribution of such change of topography and incremental changes in the static stress field, then use the results to constrain simplified models of what must have been a highly complex rupture scenario for the 1811-1812 earthquakes. It is important for the reader to note that we do not attempt to replicate the magnitude of topographic changes that occurred during the three large New Madrid earthquakes. Ground motions involved significant liquefaction through strongly non-linear processes, most likely related to near-source accelerations. These features cannot be reproduced via a linear elastic model, as we use in the present treatment. What we do propose, however, is that a simple linear elastic model is capable of generating the average spatial gradients in ground deformation.

Historical Accounts of Changes of Topography

Some eye witness accounts (mostly far-field) were compiled soon after the New Madrid earthquakes, but no comprehensive geological investigation was made until a century later (9). Prior to the earthquakes, "the country ... was formerly comprised of small prairies or meadows interspersed among the woods. Afterwards it was covered with 'slaches' (ponds) and sand hills or mounticules" (11). An eye witness to the after-effects recounts, "I have trapped there for 30 years. There is a great deal of sunken land caused by the earthquake of 1811. There are large trees ... such as grow on high land, which are now seen submerged 10 and 20 feet beneath the water" (12). Charles Lyell wrote about subterranean movements (meaning earthquakes) that control the shape of the Mississippi River, "[s]o late as the year 1812, the whole valley ... a front of three hundred miles, was convulsed to such a degree, as to create new islands in the river, and lakes in the alluvial plain, some of which were *twenty miles in extent* ? (13). This region corresponds to the north-south trending Sikeston's Ridge (Fig. 1), which subsided such that flooding developed adjacent to both east and west sides (9).

The most prominent effect of the New Madrid earthquakes was the formation of extensive swamplands and lakes, particularly west of the Bootheel lineament in the flat bottom lands of the Mississippi River, the Little River, and the St. Francis River (Fig. 1). These are Fuller's "sunk lands" and are characterized by young, wetland timber, depressed and drowned stream channels and stream banks, and lakes that grade into swamps that have hardwood stumps in their beds (9). Submergence during the 1811-1812 earthquakes created St. Francis Lake and the lakes of Hatchie Coon sunk lands farther upstream. Radiocarbon analysis of wood recovered from shallow cores within St. Francis Lake date the formation of the lake at ~200 years ago (14). Similar evidence for extensive submergence exists along the Little River (Fig. 1). Fuller (9) states that Big Lake and Lake Nicormy were formed during the New Madrid earthquakes, which is strongly supported by recent investigations of shallow bottom lake cores from Big Lake (14, 15). Lyell visited the New Madrid region 35 years after the earthquakes, before new growth and erosion had too severely obscured the effects of the earthquake, and describes the "largest area affected by the convulsion lies 8 or 10 miles westward of the Mississippi and inland from a town called New Madrid, in Missouri. It is called the "sunk country" and is said to extend along the course of the White Water (present-day Little River) and it's tributaries for a distance of between 70 and 80 miles north and south and 30 miles east and west." (16).

Much of the detailed evidence of subsidence west of the Mississippi River has been obscured by the massive drainage and waterways projects carried out in the early part of this century. Survey maps of the region made after the New Madrid earthquakes but prior to these drainage projects suggest that the extensive sunk lands ended at the eastern edge of Little River, between Big Lake and Portageville (Fig. 1) (17), just west of the Bootheel lineament.

Other isolated pockets of subsidence have been described east of the widespread sunk lands, but west of the Mississippi River. Tyronza Lake is a sunk land located 5km east of the Little River dome (Fig. 1) and Cagle Lake, prior to its drainage, lay about 10 km southwest of Little Prairie (Caruthersville) (18).

The most significant region of subsidence east of the Mississippi River involved the formation of Reelfoot Lake (19) (Fig. 1). Maps of the region made prior to 1811 show the Reelfoot River draining westward into the Mississippi River and show signs of swamp land where Reelfoot Lake now lies (20). The magnitude of subsidence is difficult to estimate because the lake is dammed to the south by the 6-10 m high Reelfoot fault scarp, the surface expression of a buried thrust fault, although it is estimated to be between 3 to 6 m (9, 21). The date of lake subsidence is known from growth rings in drowned Bald Cyprus trees to be 1812 (22).

Structural and topographic highs in the region appear less widespread than depressions, but may be simply more difficult to define because highs are more easily eroded and because they do not disrupt land-use or travel as do areas of subsidence. Nevertheless, the most prominent structural deformation in the region is the Lake County uplift (Fig. 1), a topographic and structural high of up to 10 m defined largely by deformed terraces of the Mississippi River (23) and to some extent by patterns of stream gradients across its two prominent highs, Tiptonville dome and Ridgely ridge (24). Recent uplift here is also indicated by the anomalously high sinuosity of the Mississippi River downstream of the dome (25). The northeastern boundary of the uplift is defined by the Reelfoot scarp, the surface expression of a southwest-dipping fault that underlies the uplift. This reverse fault is imaged in part by microseismicity (26) and seismic reflection profiles (27) and has been exposed by several trenches (28). Russ (23) estimates a maximum uplift of 6-10 m over the past 2300 years, some of which must have

postdated 1800, because an eye witness recounts that “keelboats used to regularly make passage

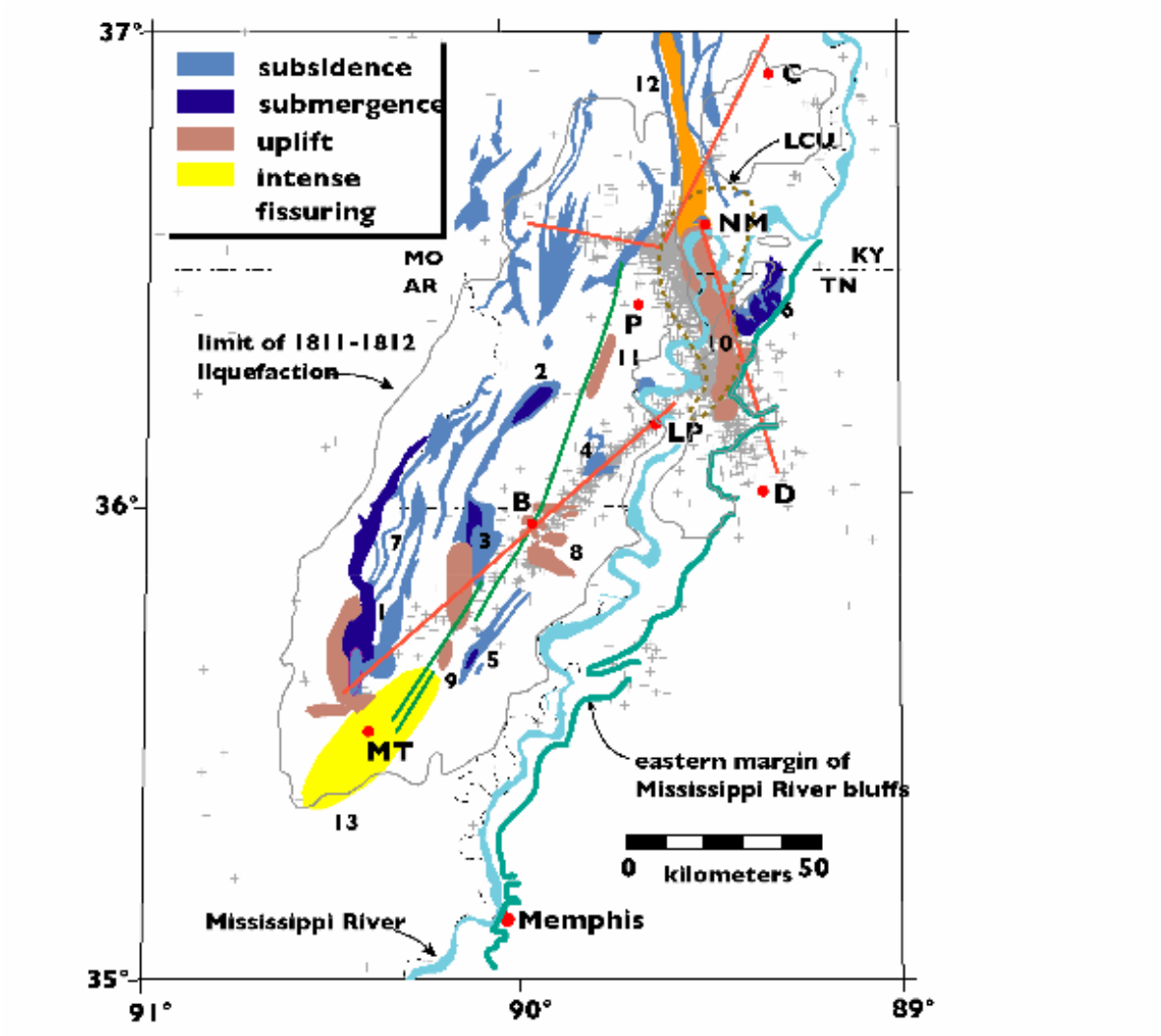

Figure 1. Distribution of uplift and subsidence due to the Great New Madrid earthquakes of 1811-1812. Data are drawn from references given in the text. NM, New Madrid; MT, Marked Tree; B, Blytheville; D, Dyersburg; C, Charleston; LP, Little Prairie (Caruthersville); P, Portageville; 1, St. Francis Lake (now River); 2, Lake Nicormy; 3, Big Lake; 4, Cagle Lake; 5, Tyronza Lake; 6, Reelfoot Lake; 7, lakes of Hatchie Coons sunk lands; 9, Little River dome; 10, Tiptonville and Ridgely ridges; 11, sand ridge; 12, Sikeston's ridge; 13, intense fissuring. Green line is the Bootheel lineament, the thick dashed line is the Lake County Uplift, red lines are fault segments.

from the Mississippi River through Portage Bayou, past the present town of Portageville, and on to the St. Francis River" (29). Following the 1811-1812 earthquakes, however, such passage was no longer possible because the land had apparently been uplifted, thus causing Portage Bayou to shallow (9). Recent investigations of Reelfoot scarp have identified several episodes of displacement across minor faults exposed in trenches (between A. D. 780 and 1000, A. D. 1260 and 1650), the most recent dated at 1812 (28, 30).

A second prominent high in the region is the Blytheville dome (9), which lies immediately to the east of the Bootheel lineament (Fig. 1) and has a maximum relief of 3-5m. The dome is defined by warping along the Left Hand Chute of Little River, but part of its boundary is also defined by meander scars of the Mississippi River, which currently flows and has since long before 1811 to the east of the dome. This led Fuller (9) to conclude that the Blytheville dome existed prior to the New Madrid earthquakes, although Russ (23) concluded from analysis of topographic maps and subsurface data that the dome is the product of natural levee deposits of the Little River and Mississippi River.

Other uplifted areas include the Little River dome, located southwest of the Blytheville dome with a relief between 1 to 3 m, which Fuller argues is probably of tectonic origin, since the "Little River meanders indiscriminately through high and low ground in a manner likely to result only from superposition or from doming of the strata beneath its established bed" (9, p. 64). A thin ridge of Pleistocene braid belt deposits, known locally as the sand-ridge runs along ~40 km of the Bootheel lineament and in part forms a west-facing scarp that defines the lineament (7, 31). The sand-ridge contains Woodland-aged (0-700 A. D.) artifacts and cultural debris from native Americans, which suggests that it existed as relatively high land prior to the 1811-1812 earthquakes. The extent to which the ridge was generated by the 1811-1812 earthquakes is unknown, although its association with the Bootheel lineament implies that it is an actively growing structure.

Rupture Scenarios

These data comprise the bulk of observational evidence to which we compare the results of numerical experiments and that we use to constrain a rupture scenario for the 1811-1812 earthquake sequence. Primary constraints on rupture scenarios are estimates of the magnitude and epicenter of each earthquake and the spatial distribution of seismicity, liquefaction, and known faults. Johnston and Schweig (32) summarize these data and state that any rupture scenario should largely be contained within the area of intense liquefaction, and should be consistent with seismicity and known faults in the region, and we concur. Seismicity in the region and the location of the prominent structural high of Lake County uplift appear to define a left-stepping, right-lateral strike-slip fault system, and a left-lateral, east-west trending fault is clearly defined to the west of New Madrid (35).

We suggest also that rupture scenarios should be consistent with (i.e., be capable of being generated by) a regional stress field that is derived from ridge push forces. The orientation of the in-situ maximum horizontal stress (which is probably close to the maximum principal stress) in the far-field is ~N60-70E (34).

At least six rupture scenarios (A-F) are permissible with these data (Fig. 2), three of which (A, C, & F) are described by Johnston and Schweig (32). Each scenario places the first New Madrid earthquake of December 16, 1811, ~**M** 8.1, on a fault defined at least in part by the

southern northeast-trending arm of seismicity (36). Scenarios A - C continue the first earthquake on the Bootheel lineament, which interpretations of shallow seismic reflections show to overlie disrupted (faulted) sedimentary units (37). Scenarios A - C also include an aftershock of estimated **M** 7.2 that occurred about 8.15 a.m. on the morning of December 16th, placed on the northern section of the southern arm of seismicity, from Blytheville, Arkansas, to Little Prairie (Caruthersville), Missouri (not shown on Fig. 2A-C). Historical accounts tell us that this aftershock was more strongly felt at Little Prairie than was the earlier mainshock (38). The third great earthquake of February 7, 1812, is placed on two of three fault segments in the central region, adjacent to the town of New Madrid and straddling the Mississippi River. The central location is constrained by eye witness accounts of waterfalls across the Mississippi River (39) and is consistent with current investigations of Reelfoot scarp, which extend its length to the northwest, crossing the meandering Mississippi River twice, upstream of modern-day New Madrid and once immediately downstream (6).

Scenarios D - F place the first mainshock on the well-defined continuous southern arm of seismicity from Marked Tree, Arkansas, to Ridgely, Tennessee, rather than the Bootheel lineament. This is in better agreement with present-day seismicity but is more difficult to reconcile with the historical accounts from Little Prairie.

Numerical Experiments

We use a three-dimensional boundary-element algorithm to calculate surface displacements in response to relative displacements across fault segments, driven by a remote uniform stress field (8). Fault ruptures are modeled as freely slipping planar discontinuities in a uniform elastic half-space. A minimum driving stress is calculated by generating and summing moment tensors for each of the rupture scenarios, and by assuming reasonable elastic constants (40). In order to generate the first earthquake of **M** 8.1, we increased the magnitude of the driving stress field by approximately 2 to 4 times the minimum derived from the moment summing. This is a consequence of the inability of finite-length, planar faults to efficiently relax the full three-dimensional strain field (41).

We first examined the capability of a given rupture sequence to be driven in such a stress field, decremented successively as each earthquake occurs. These initial experiments help discriminate likely rupture scenarios. For example, scenario F is incapable of sustaining a second mainshock of **M** > 7.4 (42) and can probably be dismissed. Scenarios A-C, in contrast to D-E, also provide an explanation for the timing of the 1811-1812 sequence. The successive changes in normal and shear stresses across rupture planes in scenarios A and C following the first mainshock, advances and delays failure across the second and third fault planes, respectively, and the second mainshock advances the third mainshock. Scenarios A-C are also consistent with the observation that the aftershock was felt more strongly at Little Prairie (Caruthersville) than was the first mainshock

Scenarios that involve the northern arm of seismicity (A, B, D, & E) are able to explain the location of the largest earthquake in the New Madrid seismic zone since 1812 (1895, ~**M** 6.6). This earthquake occurred in the tip-zone of the northern rupture, which gained strain energy following the second 1811-1812 mainshock (43). Scenario A yields the lowest maximum shear stress (~7 MPa or 70 bars) by up to a factor of nearly two (Fig. 2). That is, as deviatoric stress is generated over time, shear stress levels sufficient to drive scenario A will be reached

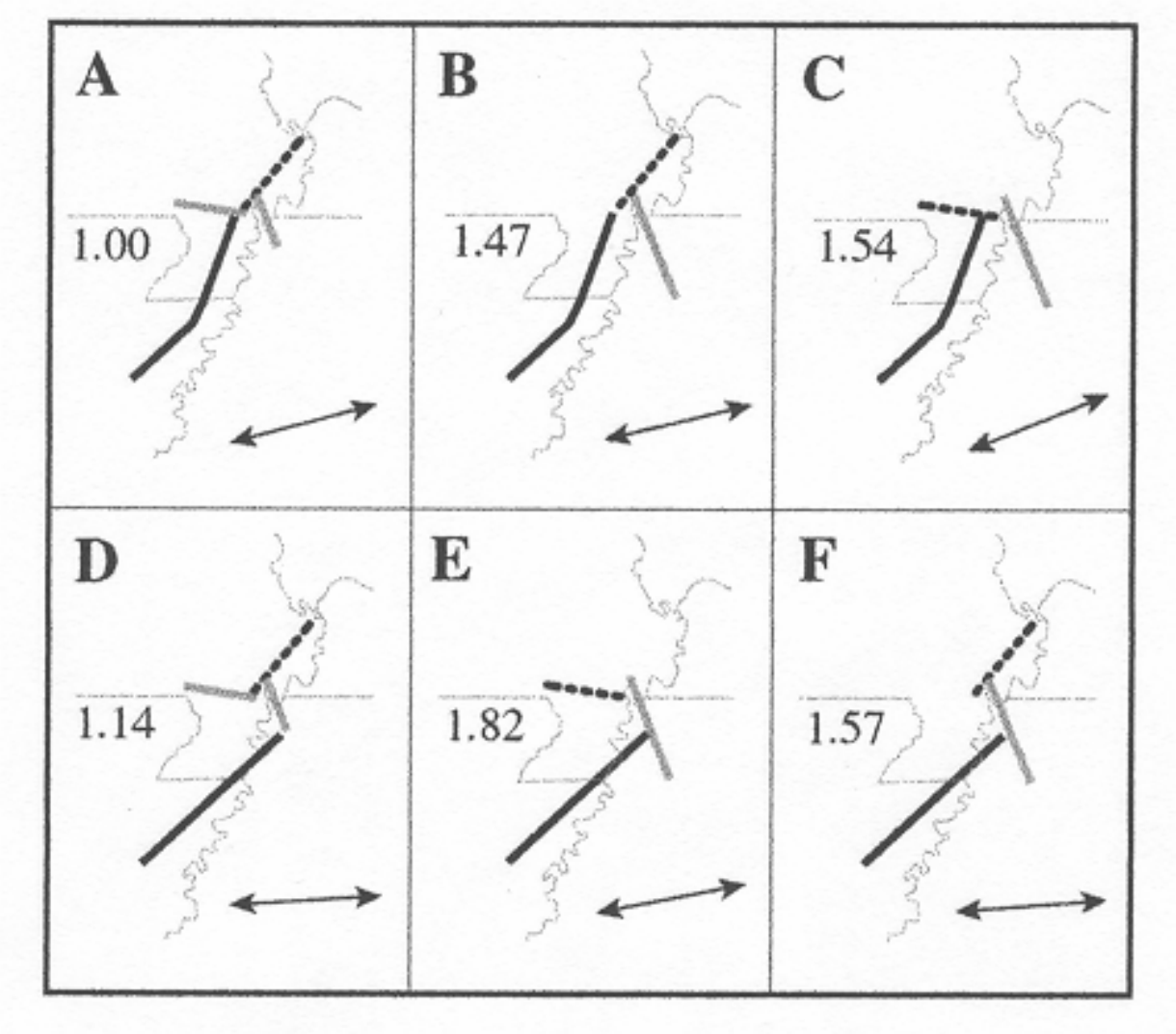

Figure 2. Six rupture scenarios for the 1811-1812 New Madrid earthquakes shown. Bold line shows mainshock of December 16, 1811, **M** 8.1; dashed line shows mainshock of January 23, 1812, **M** 7.8, gray line(s) show third mainshock of February 7, 1812, **M** 8.0 (1). The **M** ~7.2 aftershock of December 1811 is placed on the northern segment of the southern arm of seismicity, which is not shown explicitly here (but see Fig. 4) but which trends from Blytheville to Little Prairie (Fig. 1). The double-pointed arrow shows the horizontal projection of the maximum principal strain (that may be read as stress if the crust is isotropic and elastic on the time-scale over which the three earthquakes occurred), derived from moment-tensor summing (40). Scenarios A-C yield orientations that reflect the same component of the far-field in-situ stress, which is also that predicted by ridge-push forces. Scenarios D-F yield stresses that are closer to some of the local in-situ stress data, although greater scatter exists in the local and regional data (33). The number shown for each scenario is the magnitude of the maximum shear necessary to initiate the sequence of earthquakes (numbers normalized by the lowest value). Thus, if all faults shown in the scenarios exist in the upper crust, we would expect those of scenario A to rupture first, all else being equal.

earlier than for the other rupture scenarios.

These initial experiments allow us to dismiss scenario F and favor scenarios A and B over D or E, but do not provide convincing evidence for any rupture scenario. Such evidence comes from the comparison between observations of changes of topography and calculated surface vertical displacements.

The distribution of surface vertical displacements (discussed below) argue against scenarios that do not involve the Bootheel lineament (D-F) since they do not explain the observations or they generate significant surface deformation where none is reported (e.g., Fig. 3). Similar remarks may be made to parts of each of the remaining scenarios, but for reasons given above and below, we prefer scenarios that involve the northern arm of seismicity (A & B).

Scenarios A and B place the December **M** 8.1 earthquake on the Bootheel lineament and the southern segment of seismicity and a significant aftershock (not shown) on the northern section of the southern arm of seismicity. Calculated surface vertical displacements following these vertical ruptures (Fig. 4) show subsidence of the order of tens of centimeters to the immediate west of the Bootheel lineament, corresponding to the St. Francis sunklands and Big Lake (Fig. 1). Significantly, the region of predicted subsidence is bound to the east by the model Bootheel fault, which is consistent with early maps of the region (17). Significant uplift is generated to the east of and adjacent to various sections of the Bootheel lineament in scenarios A and B. Uplift associated with the change in strike of the lineament, near the Arkansas-Missouri state border, is coincident with the Blytheville and Little River domes, while adjacent subsidence to the southwest matches the unnamed area of subsidence in Figure 1. Uplift along the eastern edge of the northern Bootheel lineament corresponds well to the uplifted sand ridge. Uplift is also predicted at the southeastern tip of the mainshock, near Marked Tree, Arkansas. In this case, uplift appears to be manifest as significant fissuring associated with liquefaction (Fig. 1), an example of relatively large volume decrease that essentially proxies as uplift. Of particular significance is the generation of subsidence as a result of the aftershock and between the surface trace of the aftershock rupture and the northern Bootheel lineament. This matches the location of Cagle Lake, which appears to have formed as a result of the aftershock rather than the mainshock.

In scenarios A and B, the January 23, **M** 7.8 occurs on the shorter northern arm of seismicity, while the February 7, **M** 8.0 earthquake occurs on the central Reelfoot thrust and its western strike-slip extension (scenario A) or on its southeastern extension toward Dyersburg, Tennessee (scenario B). Both scenarios are able to explain the arcuate region of subsidence to the west of the Bootheel lineament, and significant subsidence is generated east of New Madrid, corresponding to the extensive region of young flooding observed by Lyell (16). Both scenarios also yield significant uplift across the central thrust fault, which corresponds well to the Lake County uplift (Fig. 1) in both magnitude (~4m), and symmetry (uplift increases to the northeast).

The principal difference between scenarios A and B (Fig. 5) is the extent of uplift to the west of New Madrid (scenario A) and to the southeast of the central thrust fault (scenario B). We have little evidence to distinguish between these two parts of the scenarios. No direct evidence exists of uplift north of the strike-slip extension in scenario A, although this area prior to the mainshocks was already significantly swampy, and it is possible that uplift may simply be manifest as relatively less subsidence than surrounding areas. Fuller's maps (9) indeed suggest that subsidence falls off to the north of a line corresponding to the strike-slip fault. Alternatively, geomorphology of the eastern bluffs over the southeastern extension of the central

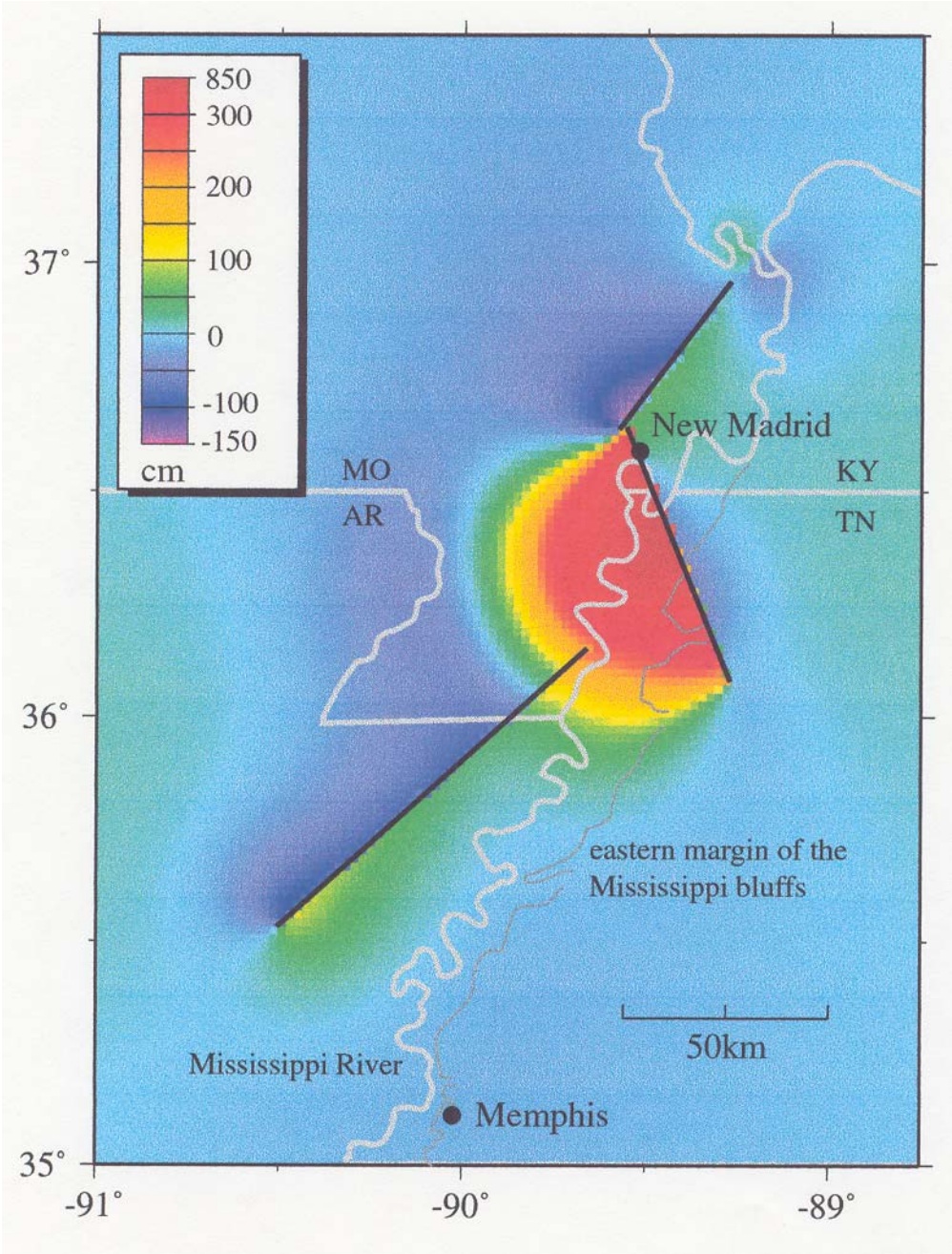

Figure 3. Calculated surface vertical displacements due to scenario F. We show this to demonstrate the inability of scenarios that do not involve the Bootheel lineament as part of the rupture sequence. Note that none of scenarios D-F can explain the subtle patterns of uplift and subsidence to the southwest of Little Prairie (e. g., Blytheville and Little River domes, sand ridge, Tyronza Lake, Cagle Lake, and concentrated subsidence at Big Lake).

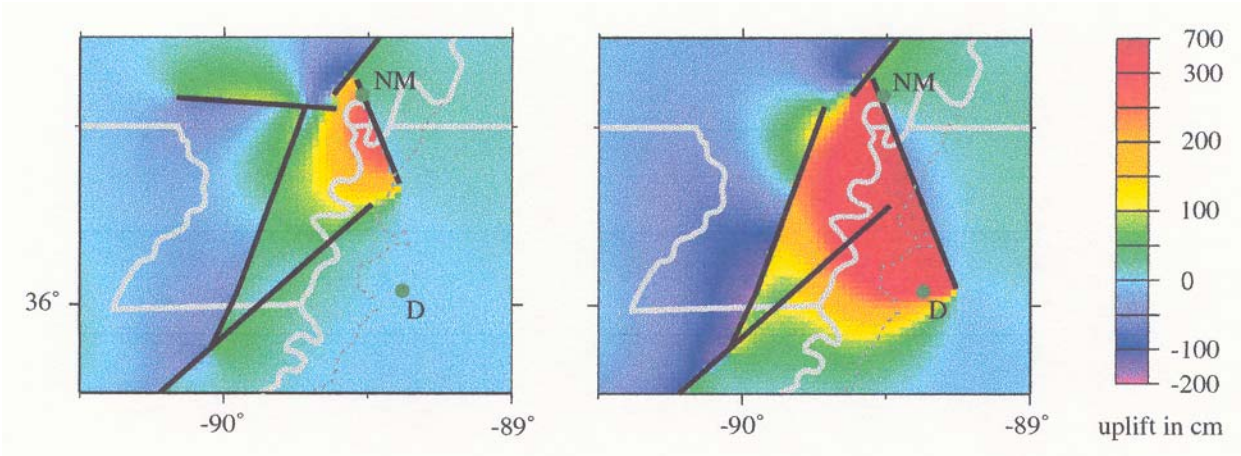

Figure 4. Calculated surface vertical displacements due to scenarios A (left) and B (right). Note that the aftershock occupies the northern segment of the southern arm of seismicity, which is not explicitly shown on Fig. 2). Distance and displacement scales are the same for each figure. The most significant difference between the two scenarios is the extent of significant uplift to the southeast of the central thrust. No significant evidence is known to suggest uplift to the southeast of the same order of magnitude as that clearly observed in the central thrust zone, but see ref. 44.

thrust is consistent with relative uplift and subsidence to the southwest and northeast, respectively, of the fault (44).

Subtle uplifts of this magnitude, giving rise to slope increases ~10^{-3}, may have a profound effect on the behavior of major rivers such as the Mississippi, which has an average slope of ~10^{-4} (45). Lake County uplift is associated with anomalously greater sinuosity of the Mississippi River meander (25), which is probably a reflection of both increased slope and greater resistance of uplifted clay-rich horizons following the mainshocks (23). A similar increase of sinuosity occurs to the north of the confluence of the Mississippi and Ohio Rivers at Thebes Gap (Fig. 1), coincident with uplift associated with the tip zone of the northern strike-slip fault (Fig. 6). The Mississippi River may also be guided in its course farther south as it leaves the Lake County uplift and heads south. There the river appears to track the eastern side of the modern floodplain, and has done so for at least 10,000 years (46), influenced in this course perhaps by the eastward sloping surface predicted by rupture scenario A (Fig. 6).

The cumulative results from both static-stress and change-of-topography numerical experiments strongly suggest that the most likely rupture scenario for the 1811-1812 earthquakes involves the Bootheel lineament, or what should probably be referred to now as the Bootheel fault, the central Reelfoot thrust, and the northern arm of seismicity. The Bootheel fault, at least its well-defined northern section, is comparatively aseismic, similar in this sense to largely aseismic segments of the San Andreas fault that sustained large magnitude earthquakes in 1857 and 1906 (47).

Some of the features described here, in particular the sand ridge, Blytheville and Little River domes, and Lake County uplift, existed in some form prior to the New Madrid earthquakes, which suggests that the rupture scenario preferred here was repeated during an earlier set of earthquakes. This is consistent with the extensive paleoliquefaction investigations in the New Madrid region, which are now showing widespread strong ground shaking events have occurred at least three times in the past 2000 years (2). Nevertheless, repeated earthquakes in the New Madrid must be relatively limited; that is, the system is probably fairly young, since both topography and finite deformation is generally quite subtle (4, 48).

In conclusion, the structural setting of the New Madrid faults may more firmly be recognized as a relatively large left-stepping, right-lateral strike-slip system that is being linked or smoothed by the Bootheel fault. This fault pattern accommodates a regional strain that is consistent with the orientation of ridge-push forces, and the local in-situ stresses arise probably as a result of residual or accumulating strains.

Notes and references

1. A. C. Johnston, *Geophys. J. Int.* **126**, 314-344 (1996).

2. M. P. Tuttle, E. S. Schweig, *Geology* **23**, 253-256 (1995); M. P. Tuttle, E. S. Schweig, *J. Geophys. Res.* **101**, 6171-6178 (1996).

3. Recent measurements by Neuman et al., (Neuman, A., Stein, S., Weber, J., Engeln, J., Mao A., and Dixon, T., *Science* **284** 619-621, 1999) show that the 2-sigma error remains larger than the current measured relative velocities, which means that either the ground is not deforming or

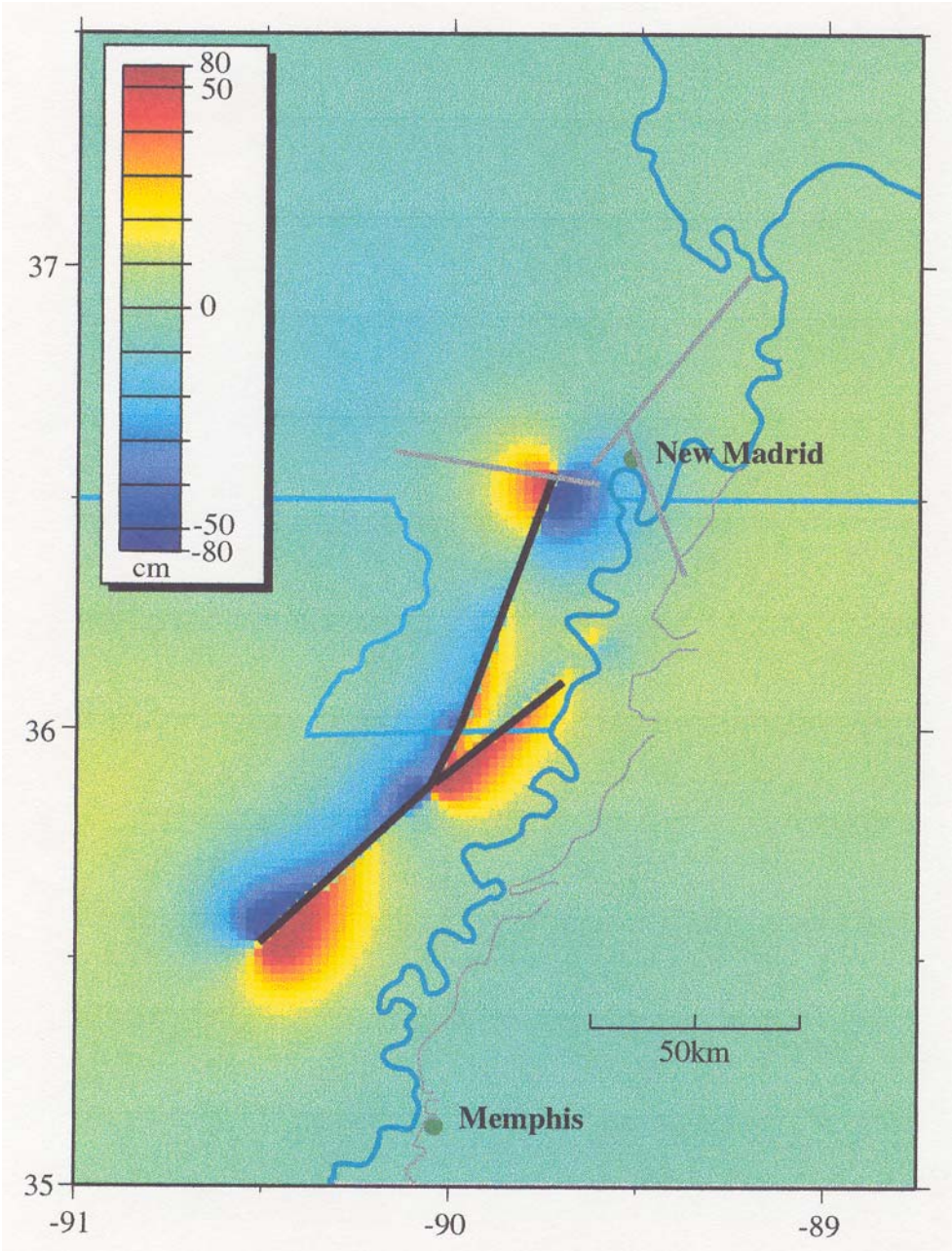

Figure 5. Calculated surface vertical displacements due to the first mainshock and aftershock of scenario A. Note that these two earthquakes are able to well explain the subtle patterns of uplift and subsidence to the southwest of Little Prairie, including the Blytheville and Little River domes, uplift of the sand ridge along the eastern side of the Bootheel lineament, Tyronza Lake, Cagle Lake, and concentrated subsidence at Big Lake.

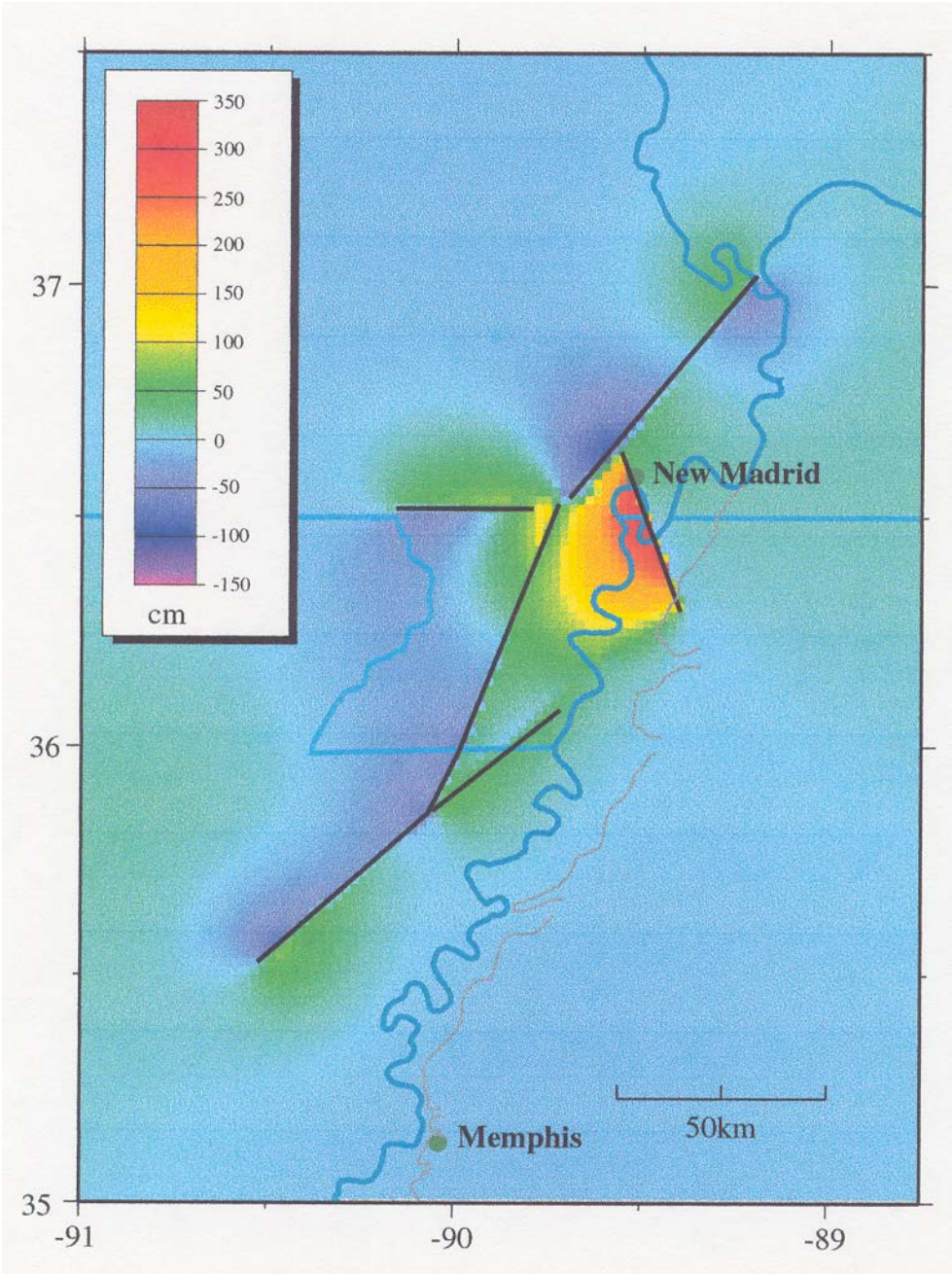

Figure 6. Calculated surface vertical displacements due to scenario A. Scenario explains the generation of virtually all presently known regions of uplift and subsidence summarized in Fig. 1 with the exception, possibly, of uplift to the north of the western part of the third mainshock. This area prior to the mainshocks was already significantly swampy, and it is possible that uplift may simply be manifest as relatively less subsidence than surrounding areas, consistent with the observation that subsidence falls off to the north of a line corresponding to the strike-slip fault (9).

that measurement errors are simply too large.

4. E. S. Schweig, M. A. Ellis, *Science* **264**, 1308-1311 (1994).

5. P. Somerville and C. Saikia, Ground motion attenuation relations for the central and eastern United States, Final Technical Report to USGS, NEHRP, http://erp-web.er.usgs.gov/reports/annsum/vol42/cu/cu_vol42.htm., 2000. McGarr, A. and Fletcher, J. B., Maximum slip in earthquake fault zones, apparent stress, and stick-slip friction, BSSA, 93, p2355-2362, 2003.

6. R. B. Van Arsdale, K. I. Kelson, C. H. Lumsden, *Seismol. Res. Lett.* **66**, 57-62 (1995).

7. E. S. Schweig, III, R. T. Marple, *Geology* **19**, 1025-1028 (1991); E. S. Schweig, III, R. T. Marple, Y. Li, *Seismol. Res. Lett.* **63**, 277-284 (1992).

8. J. Gomberg, M. Ellis, *J. Geophys. Res.* **99**, 20,299-20,310 (1994).

9. M. L. Fuller, *U.S. Geol. Surv. Bull. 494* (1912).

10. J. L. Penick, Jr., *The New Madrid earthquakes* (University of Missouri Press, Columbia, Missouri, ed. revised, 1981).

11. L. Bringier, *American Journal of Science and Arts* **3**, 15-46.

12. A. N. Dillard, in *The Mississippi Valley, its physiography* J. W. Foster, Ed. (Chicago, 1869) pp. 19-22.

13. C. Lyell, *Principles of geology* (John Murray, London, 1830), vol. I.

14. M. J. Guccione, J. Q. Miller, R. B. VanArsdale, *Geol. Soc. Am. Abstr. Prog.* **26**, 7 (1994).

15. M. J. Guccione, R. B. VanArsdale, L. H. Hehr, *Geol. Soc. Am. Abstr. Prog.* **25**, A-460-461 (1993).

16. C. Lyell, *Principles of geology* (John Murray, London, ed. 11, 1871), vol. I.

17. O. Kochtitzky, *Map of the lowlands of southeast-Missouri*. (Little River Drainage District, Cape Girardeau, Missouri, 1903).

18. C. Chapman, L. O. Anderson, *Mo. Arch.t* **17**, 1-140 (1955); M. J. O'Brien, *Cat monsters and head pots: the archeology of Missouri's Pemiscot Bayou* (University of Missouri Press, Columbia, Mo., 1994). Mr. Cagle, a homesteader, is cited as an eye witness to the formation of the lake during the earthquake sequence, although the specific timing is unknown.

19. R. B. Van Arsdale, D. W. Stahle, M. K. Cleaveland, M. J. Guccione, *Geology* **26**, 515-518

(1998).

20. S. C. Williams, *The beginnings of western Tennessee* (Watauga Press, Johnson City, Tennessee, 1930); L. C. Glenn, *J. Tenn. Acad. Sci.* **8**, 2-12 (1933).

21. D. P. Russ, *Geol. Soc. Am. Bull., Part I* **90**, 1013-1018 (1979).

22. D. W. Stahle, R. B. VanArsdale, M. K. Cleaveland, *Seismol. Res. Lett.* **63**, 439-448 (1992).

23. D. P. Russ, *U.S. Geol. Surv. Prof. Pap. 1236-H* (1982).

24. D. Merritts, T. Hesterberg, *Science* **265**, 1081-1084 (1994).

25. K. F. Boyd, S. A. Schumm, *U.S. Geol. Surv. Prof. Pap. 1538-R* (1995).

26. J. M. Chiu, A. C. Johnston, Y. T. Yang, *Seismol. Res. Lett.* **63**, 375-393 (1992); J. Pujol, A. Johnston, J. M. Chiu, Y. T. Yang, *Engineering Geology* (in press). Microseismicity suggests the fault is discontinuous across the intersection with the southern arm of seismicity.

27. J. L. Sexton, P. B. Jones, *Geophysics* **51**, 1760-1788 (1986); E. W. Woolery, R. L. Street, Z. Wang, J. B. Harris, *Geophys. Res. Lett.* **20** (1993); E. W. Woolery, W. Zhenming, R. L. Street, J. B. Harris, Seismol. Res. Lett. **67**, 67-74 (1996).

28. K. I. Kelson, G. D. Simpson, R. B. Van Arsdale, C.C. Haraden, W. R. Lettis, *J. Geophys. Res.* **101**, 6151-6170 (1996).

29. G. C. Broadhead, *The American Geologist* **30**, 76-87 (1902).

30. K. I. Kelson, R. B. VanArsdale, G. D. Simpson, W. R. Lettis, *Seismol. Res. Lett.* **63**, 349-356 (1992).

31. W. J. Autin, D. J. McCraw, J. I. Snead, J. M. Kruger, Surface geologic mapping of part of the Bootheel lineament area: A pilot project in the New Madrid seismic zone, *Final report to the U.S. Geological Survey* (1995).

32. A. C. Johnston, E. S. Schweig, *Annual Review of Earth and Planetary Sciences* **24**, 339-384 (1996).

33. M. L. Zoback, M. D. Zoback, *J. Geophys. Res.* **85**, 6113-6156 (1980); M. L. Zoback, M. D. Zoback, in *Geophysical framework of the continental United States* L. C. Pakiser, W. D. Mooney, Eds. (Geological Society of America Memoir 172, Boulder, Colorado, 1989) pp. 523-539.

34. R. M. Richardson, *J. Geophys. Res.* **97**, 11,739-11,748 (1992).

35. A strike-slip fault is suggested by the microseismicity (26) and a left-lateral sense by its conjugate orientation with respect to the northeast trending right-lateral faults and by the focal mechanism of the 1991 Risco, **M**4.3 earthquake [S. C. Chiu, H. Wang, J. M. Chiu, A. Johnston, *Seismol. Res. Lett.* **62**, 166-167 (1991)].

36. We place the first earthquake here because historical accounts from New Madrid say shocks came from the south, and reports from Arkansas Post indicate shocks came from the northeast [J. Ritchie, *Ann. Rep. Board of Regents of the Smithsonian Inst.* (Harris, Washington, D.C., 1859), pp. 421-424].

37. E. S. Schweig, III, et al., *Seismol. Res. Lett.* **63**, 285-296 (1992).

38. Historical accounts from Little Prairie report the first mainshock as the "distant earthquake" as compared to the first aftershock;.Little Prairie was badly damaged by the aftershock and abandoned [G. Lesieur, *Campbell's Gazetteer of Missouri* (R. A. Campbell, St. Louis, Mo., 1874) p. 394; W. L. Pierce, Letter dated December 25, 1811 in *New York Evening Post,* 11 Feb. 1812 issue(1812); J. Fletcher, Narrative dated January 21, 1812 in *Pittsburg Gaz.,* 14 Feb. issue (1812)].

39. M. Speed, "Letter dated March 3, 1812," *Pennsylvania Gazette*, March 18, 1812.

40. Moment tensors were obtained for each rupture by taking the strike, dip, and slip vector (assumed to be either pure strike-slip or pure dip-slip), the seismic moment, [T. C. Hanks, H. Kanamori, *J. Geophys. Res*. **84**, 2348-2350 (1979)], and a volume corresponding to 250 km x 100 km x 33 km. The seismic strain tensor , where *u* and *n* represent fault slip vectors and normals respectively (Kostrov, V. V., *Izv. Acad. Sci. USSR Phys. Solid Earth* **1**, 23-44, 1974). *i* and *j* = 1,2,3. We use a Young's modulus of 70 GPa and a Poisson's ratio of 0.25 to convert strains into stresses, assuming an isotropic elastic constitutive relation.
$Mo = 2/3 \log Mw - 10.7$ $e_{ij} = 3M^*_{ij}/2mV$ $M^*_{ij} = Mo(u_i n_j + u_j n_i)$

41. Strains obtained by moment summing represent the strain that earthquakes accommodate or relax, which is the minimum of the total deviatoric strain present in the crust at the time of the earthquakes. Therefore, the stress field derived from these strains represents the minimum necessary to drive these ruptures. It is to be expected that a greater stress field will be required to generate the earthquakes, since the faults are finite in length and do not sample the space homogeneously. In other words, the faults cannot completely tap the entire strain energy available.

42. In order to sustain an earthquake of **M**>7.4 the model-fault rupture in scenario E is required to have a length L>60 km, which appears unlikely from the distribution of microseismicity.

43. Ellis, M., Schweig. E. S., Prejean, S. G. and Johnston, A. C. *EOS Trans. Am. Geophys. U.*, **76**, F381, 1995. The second largest earthquake in the region since 1812 (1843, ~**M** 6.2) similarly occurred in a zone of increased shear strain energy south of the first mainshock. Similar spatial relations between increased shear stress and subsequent earthquakes have been

noted along strike-slip fault systems elsewhere, most notably during the sequence of earthquakes that led up to the 1992 Landers **M** 7.3 event [Stein, R. S., King, G. C. P. and Lin, J., *Science*, **258**, 1328-1332, 1992] and earthquakes along the North Anatolian fault zone [Stein, R. S. and Barka, A. A., *EOS Trans. Am. Geophys. U.* , **76**, F533, 1995].

44. Van Arsdale, R. B., Cox, R. T., Johnston, A. C., Stephenson, W. J., and Odum, J. K., Southeastern extension of the Reelfoot Fault, *SRL*, **70**, 348-359, 1999. Also, peak bluff elevations measured at half-km intervals from Memphis, Tennessee, to the Kentucky border, show the bluffs as anomalously high and low over sites that correspond to the hanging wall and footwall, respectively. Similarly, streams over the hanging wall bluffs appear more deeply entrenched than those over the footwall bluffs, which are commonly infilled as if base level has locally risen.

45. C. Paola and D. Mohrig, *Basin Research*, **8**, 243-254, 1996

46. R. T. Saucier, *Geomorphology and Quaternary geologic history of the lower Mississippi Valley* (U.S. Army Engineer Waterways Experiment Station, Vicksburg, Mississippi, 1994), vol. 1.

47. The 1857 **M** 8.1 earthquake in central California occurred on the Fort Tejon segment of the San Andreas fault and the 1906 **M** 7.8 San Francisco earthquake occurred along the central and northern section of the San Andreas fault. Both of these segments are largely aseismic today.

48. T. L. Pratt, *Seismol. Res. Lett.* **65**, 172-179 (1994).

Summary of Parts 1 and 2

The northern Mississippi embayment has a rather complex history including late Precambrian and Cambrian rifting, Paleozoic deformation not discussed here (i.e. formation of the Blytheville arch), a Hot Spot origin in Late Cretaceous, minor Paleocene Reelfoot rift subsidence, compressional faulting and the formation of a north trending 100 m deep by 50 km wide trench during the Eocene, and Quaternary compressional faulting (Figs. 3-5 and 9 of Part 1). The western margin of the Eocene trench is coincident with the Blytheville arch and southern portion of the New Madrid seismic zone. Thus, it appears that much of the New Madrid seismic zone is coincident with a Paleozoic arch that was reactivated during Eocene compression. The structure contour map of the top of the Eocene/base of the Mississippi alluvium (Fig. 6 of Part 1) reveals areas of Late Wisconsin to present subsidence and uplift that we believe reflects coseismic deformation accumulated over many earthquake cycles.

A three-dimensional boundary-element algorithm was used to compare six faulting scenarios (A through F) with coseismic deformation during the great New Madrid earthquakes of 1811-1812 (Figs. 1 and 2 of Part 2). Scenario A best fits the coseismic deformation. Scenario A locates the December 16, 1811 main shock on the Bootheel fault (lineament), the December 16 aftershock along the northern section of the southern arm of seismicity from Blytheville, Arkansas, to Little Prairie (Caruthersville), Missouri, the January 23, 1812 earthquake on the

unnamed fault trending northeast from New Madrid, Missouri, and the February 7, 1812 earthquake on the Reelfoot thrust fault and its strike slip western extension. When comparing Figure 6 of Part 1(Eocene top) with Figure 6 of Part 2 (Scenario A) it is apparent that the map of the deformed top of the Eocene (interpreted to reflect Late Wisconsin to present deformation) fits faulting Scenario A quite well. Starting at the northern portions of these two figures a number of topographic low and high areas are common to both figures: 1) the low immediately east of the northernmost fault near the confluence of the Mississippi and Ohio Rivers, 2) the low immediately northwest of the New Madrid river bend, 3) the high area trending westerly from the New Madrid bend, 4) the high coincident with the Lake County uplift, 4) the low along the northwest side of the Bootheel fault, and 5) the high on the southeast side of the Bootheel fault and Blytheville arch. Although the top of the Eocene map in general matches Scenario A there are two areas that do not match. The subsidence of the Reelfoot Lake basin on the top of the Eocene is not captured in Scenario A. The second area that does not correspond is the area immediately east of the Bootheel lineament and west of the southern portion of the Lake County Uplift. At this location, the top of the Eocene is low but Scenario A shows it as a high. However, it is interesting that Figure 5 of Part 2 does show a low in this general area.

We believe that this study has contributed significantly to our understanding of the tectonic history and 1811-1812 fault sequence of the New Madrid seismic zone. By combining the subsurface geology, geomorphology, and three-dimensional boundary-element modeling we believe that Scenario A is the best model for the 1811-1812 sequence. The differences between the top of the Eocene map and Scenario A may be due to insufficient drill hole data to adequately define the top of the Eocene, very recent initiation of the Bootheel fault, or that some adjustment to Scenario A is needed. The fact that there are only minor differences between the Late Wisconsin to present deformation and 1811-1812 coseismic deformation suggests that Scenario A has been occurring since initiation of the New Madrid seismic zone probably in the Quaternary. The close correspondence of the top of the Eocene and Scenario A maps also suggests that future earthquake sequences and coseismic deformation will continue to follow the same spatial pattern.